Ultracentrifuge Studies with Absorption Optics. IV. Molecular Weight Determinations at the Microgram Level*

H. K. Schachman and S. J. Edelstein

ABSTRACT: Recognition of the value of the absorption optical system for ultracentrifugal analysis has stimulated the development in recent years of an automatic split-beam photoelectric scanning optical system. This apparatus in conjunction with a monochromator incorporated in the base of the ultracentrifuge has proven to be capable of discriminating among various chemical species during ultracentrifuge experiments. At the same time it provides a convenient method for following the transport or redistribution of solute molecules in both sedimentation velocity and equilibrium experiments. This paper describes modifications in the instrument aimed at enhancing the linearity, sensitivity, and accuracy of the recording system. The changes in design include a power supply for the logarithmic convertor, a servo mechanism for controlling the photomultiplier voltage so as to produce a constant output for the solvent cell, appropriate circuitry to permit the analysis of the two samples in a single ultracentrifuge experiment, an electrical attenuator to permit the absolute measurement of optical densities, and adjustable masks for the elimination of stray light. Numerous tests of the electronic circuits and optical system are described to illustrate the accuracy, linearity, and spectral range of the recording system for the absolute measurement of solute concentrations. Data are presented showing that measurements can be made satisfactorily at 230 mμ and optical densities of 0.02 are sufficient for quantitative sedimentation experiments. Studies with bovine plasma albumin involving the combined use of the photoelectric scanner and the Rayleigh interferometer not only demonstrate the linearity of the response of the scanner but also permit the determination of extinction coefficients during ultracentrifuge experiments. With light of wavelength 230 mμ it was possible to measure the sedimentation coefficient of aspartate transcarbamylase at concentrations as low as 3 μg/ml. The value, 11.7 S, indicates that this enzyme does not dissociate into subunits even at these very low concentrations. Sedimentation equilibrium studies are presented to illustrate the application of the scanner for a variety of biochemical problems. These include molecular weight determinations of a homogeneous solute, adenosine, and a paucidisperse sample of bovine plasma albumin. Both low- and high-speed sedimentation equilibrium experiments are described. Molecular weight measurements of bovine plasma albumin were made from data corresponding to concentrations of only about 4 μg/ml. The utility of the scanner is shown by a study of aldolase subunits in solutions containing guanidine hydrochloride at high concentrations. Preliminary data are presented which permit the evaluation of preferential interactions in these multicomponent systems. From these results molecular weights are calculated confirming earlier conclusions that aldolase is composed of three polypeptide chains. Finally the scanner was employed for an examination of the association–dissociation behavior of oxyhemoglobin in a dilute, neutral buffer. The results show that the four-chain hemoglobin molecules dissociate into single polypeptide chains at concentrations about 2 μg/ml.

A considerable amount of the research with the ultracentrifuge during the past 10 years has been made possible by the reintroduction of the absorption optical system in the form devised originally by Svedberg and his colleagues (Svedberg and Pedersen, 1940). This renewed interest in the prematurely discarded absorption optical system stemmed from its inherent sensitivity as compared to refractometric and interferometric optical techniques (Shooter and Butler, 1956; Schumaker and Schachman, 1957) as well as its capacity for discriminating among chemical species on the basis of differences in absorption spectra (Schachman, 1959). Accompanying this surge in the popularity of absorption optics for the study of biological macromolecules in the ultracentrifuge has been the development of automatic, photoelectric scanning systems which produce directly traces of the distribution of the light-absorbing molecules in the ultracentrifuge cell (Schachman, 1960; Aten and Schouten, 1961; Hanlon *et al.*, 1962; Lamers *et al.*, 1963; Deschepper and Van Rapenbusch, 1964; Spragg *et al.*, 1965; Van Rapenbusch and Deschepper, 1966). By means of these scanners not only were the tedious procedures associated with the photographic method eliminated but also

* From the Department of Molecular Biology and Virus Laboratory, University of California, Berkeley, California. *Received April 6, 1966.* This research was supported in part by U. S. Public Health Service Research Grant from the National Institute of General Medical Sciences, GM-12159, by National Science Foundation Research Grant G-10795, and by a contract between the Office of Naval Research and the Regents of the University of California.

essentially direct viewing of the sedimentation process was achieved.

In the first version of the apparatus developed in this laboratory, direct plots of optical density *vs.* distance were produced by the use of a data-sampling technique. This converted the light pulses received by the photomultiplier into a continuous function representing the logarithm of the intensity of the transmitted light as a function of position in the ultracentrifuge cell (Hanlon *et al.*, 1962). For many types of sedimentation experiments this scanning technique proved satisfactory, but imperfections in the optical system precluded its use for accurate sedimentation equilibrium studies. Since the limitations with the single-beam scanner stemmed from the optical system rather than from the detecting and recording method, it appeared necessary for precise work to monitor the optical system and to correct continuously for optical defects. Accordingly, in a subsequent design (Lamers *et al.*, 1963) the basic principle of double-beam spectrophotometers was incorporated. In this way corrections were made automatically for imperfections in the optical system such as reflections from surfaces and variable scattering from oil and dust deposits which accumulated on the optical components during prolonged operation of the ultracentrifuge. Nonuniform illumination and fluctuations in light intensity also were compensated for directly. This latter system, though using only a single light beam, simulated double-beam operation by employing the rotor as a light chopper causing first one compartment of the cell containing the solvent to appear in the light path and then the other which was filled with solution. By storing the voltage generated by the first light burst and then comparing it with that produced by the light transmitted by the second compartment it was possible to obtain the optical density of the solution relative to the solvent. This was done continuously while the photomultiplier was moved progressively across the image of the ultracentrifuge cell.

Although the split-beam photoelectric scanning system functioned effectively for many types of sedimentation experiments (Schachman, 1963a,b) limitations in the instrumentation were apparent, and many of the problems have now been remedied in subsequent work described herein. In particular, efforts have been directed toward improving the linearity and accuracy of the recording system so that it could be employed routinely for precise determinations of molecular weights by sedimentation equilibrium experiments. This has necessitated modification of both the electronic circuitry and the mechanical transmission for driving the photomultiplier across the image. These alterations have led to a more versatile instrument capable of analyzing two samples simultaneously and operating accurately with much greater sensitivity. Experiments can now be performed routinely with light having wavelengths as low as 225 mμ and with solutions having an absorbance of only 0.02. The basic modifications of the photoelectric split-beam scanning absorption system are described in this paper along with a series of sensitive tests of the electronic components, individually and as a complete recording system. Emphasis was directed toward assessing the fidelity of the optical system for the measurement of optical densities. These experiments demonstrated that absolute concentrations of proteins and other solute molecules can be measured simply and accurately during ultracentrifuge experiments; accordingly a series of sedimentation studies was initiated to test the sensitivity of the photoelectric scanning system. Among these studies were sedimentation velocity experiments at concentrations of only 3 μg/ml. In addition sedimentation equilibrium experiments were conducted on small molecules and proteins. Accurate molecular weights were obtained from data at concentrations of only 3–10 μg/ml. These studies were then extended to multicomponent systems containing high concentrations of a third component such as guanidine hydrochloride[1] or sodium chloride. Finally the utility of the scanner was illustrated by analysis of the association–dissociation behavior of oxyhemoglobin in the concentration range from 2 μg/ml to 0.4 mg/ml.

Design and Construction of Multiple-Cell Split-Beam Photoelectric Scanner

General Considerations. In the design of a split-beam photoelectric-scanning apparatus for use with conventional ultracentrifuge rotors two different arrangements may be envisaged for the placement of the solvent and solution. One of these employs a double-sector cell with the solvent and solution in separate compartments and an opaque counterbalance cell (with reference holes) in the opposite cell hole in the rotor. Alternatively the solvent and solution are placed in separate single-sector cells which are located 180° apart in the elliptically shaped ultracentrifuge rotor. For both of these arrangements the system must include holding circuits for the reference (solvent) and sample (solution) pulses, a logarithmic convertor to permit direct recording of optical densities, and an electronic switch for separating the light pulses and routing the signals to the appropriate holding circuits and then to a difference amplifier where subtraction is performed.

With both of these arrangements a reliable method is required for detecting which cell (or compartment) is responsible for each burst of light as the cells move by the optical path. When double-sector cells are employed the detecting technique is based directly on the information received by the scanning photomultiplier itself. Identification of the reference and sample cells can be deduced unambiguously from the time dependence of the light bursts. As the rotor turns, the photomultiplier receives no light until the double-sector cell crosses the light beam. While the cell moves past the optical path two short bursts of light strike the photomultiplier in quick succession. Following

[1] Abbreviations used: G-HCl, guanidine hydrochloride; BPA, bovine plasma albumin; ATCase, aspartate transcarbamylase; BrCTP, bromocytidine triphosphate.

this is a long dark period as the rotor makes a complete revolution. By appropriate filling of the compartments of the double-sector cell in terms of the rotational sense of the rotor the first light burst after the long dark period can be made to represent the transmittance of the solvent and the second (after the short dark period) to correspond to the solution. Switching and routing the signals from the light pulses proved to be flawless for this arrangement of solvent and solution (Lamers *et al.*, 1963). The first signal from the photomultiplier (after the long dark period) was fed into a logarithmic convertor and then directed to a reference holding circuit where it was stored as the logarithm of the light intensity. At the same time the decrease in light intensity at the trailing end of the first pulse activated a switch closing the gate to the reference holding circuit and simultaneously opening the gate to the second (or sample) holding circuit where the second pulse was stored as the logarithm of the transmittance of the solution. The gating circuit which functioned as a switch was designed so that after a fixed (but adjustable) period the circuitry automatically returned to its original form, thereby causing the first pulse after the long dark period to pass to the reference holding circuit. In this way the photomultiplier voltages produced by the two bursts of light were not only distinguished but they were routed unambiguously to the proper holding circuits as the logarithmic values of the respective signals.

When the solvent and solution are placed in cells opposite one another in the rotor, the sequences of light and dark periods are identical for both cells. Thus the light pulses corresponding to the solvent and solution cannot be distinguished simply, and the switching mechanism described above for double-sector cells cannot be used. An independent sensing element is required, therefore, in order to detect the rotor position and activate the switching mechanism at the proper time. The introduction of additional photoelectric components is accompanied by delicate alignment problems. Despite these complications this system possesses certain advantages which are discussed here prior to a description of the auxiliary sensing element and the modified electronic circuitry.

The signal generated by the photomultiplier is proportional to the level of light incident on the photocathode. Thus a long slit should be used in front of the photocathode. However, the slit length at the photomultiplier must be sufficiently short that the photomultiplier cannot "see" both cells at the same time. With double-sector cells this is a serious limitation, for the slit length must be no greater than the image of the central rib which separates the two compartments of the cell. As a consequence the length of the slit at the photomultiplier has been only about 2 mm (Lamers *et al.*, 1963). In effect this restriction has proved costly since the photocathodes of the photomultipliers now in use have a diameter of 10 mm. If a full-length slit could be employed in the photomultiplier assembly, the output signal would be increased fivefold for the same prevailing light level in the image. With this arrangement the system could be operated with much smaller voltages on the photomultiplier thereby leading to traces more nearly noise free with a consequent gain in precision. Alternatively, with a longer photomultiplier slit the sensitivity of the scanner would be enhanced thereby permitting measurements to be made at lower total light levels than used heretofore. In this way studies could be conducted with light of wavelengths in the far-ultraviolet region of the spectrum.

When two single-sector cells are employed, with solvent in one and solution in the other, the slit at the photomultiplier can have a length equal to the diameter of the photocathode itself. With the cells separated by 180°, the dark period between solvent and solution pulses would be of long duration (500 μsec for a rotor turning at 60,000 rpm contrasted to 5 μsec for a double-sector cell). As a consequence there are no phasing problems in separating the light pulses. By the time the solution cell has moved into the optical path the solvent cell is completely out of the light beam and there is no difficulty with the photomultiplier "seeing" both cells simultaneously. To exploit this increase in the length of slit at the photomultiplier, special single-sector cells having a large sector angle should be used. In this way much more light would strike the photomultiplier in each light burst and the output singals would be much greater. Two sets of cell windows would be required with this arrangement as contrasted to the single pair of windows used with double-sector cells. This has proved not to be a disadvantage, however. Since the transmittance of the quartz or sapphire windows now available has been uniformly high even at wavelengths below 230 mμ, the split-beam scanner can function effectively with the solvent and solution in individual cells separated by 180°.

In pursuit of this goal of enhanced sensitivity, the split-beam scanner described earlier (Lamers *et al.*, 1963; Schachman, 1963a) was modified so as to incorporate the desirable features outlined above while still preserving the virtues of the original design. This furnished an opportunity to increase the stability and linearity of the recording system and to incorporate provisions for the absolute measurement of optical densities. In addition the electronic circuits were modified so as to exploit the external sensing element and permit simultaneous operation with two double-sector cells. By this means in a single experiment two different solutions can be examined relative to the two solvents. Many of the design features are similar to those in the earlier version of the split-beam scanner constructed in this laboratory. Therefore, only those aspects peculiar to multiple cell operation are presented here along with a set of sensitive tests and criteria for satisfactory performance of the instrument for sedimentation equilibrium experiments. Details of the circuits and electronic components are given elsewhere (Lamers, 1965), and the principles elaborated in this work have since been applied (Cheng and Littlepage, 1966) for the construction of a photoelectric scanner

capable of analyzing six samples in a single experiment.

Multiple Cell Operation. Figure 1 is a block diagram illustrating the important components in the multiple-cell split-beam scanner. Some are mounted directly on the ultracentrifuge, the section indicated by a, whereas the remainder, b, are contained in a separate console unit. With two double-sector cells in the rotor and the photomultiplier-slit assembly stationed along the image at a position corresponding to a specific level in the cells, four discrete light pulses strike the photocathode during each revolution of the rotor. These pulses arrive in pairs with the first in each pair representing the solvent and the second the solution. Each of these light bursts, having a duration less than 1% of the time of one revolution, must be separated, fed through the appropriate circuitry, and recombined with other pulses from the same sector as well as those from its "mate" to form the profile of interest. Nothing in this train of pulses distinguishes one pulse pair from another; nevertheless each pulse must be identified with the sector responsible for it. This was facilitated by supplementing the pulses received by the scanning photomultiplier with an auxiliary light pulse striking a stationary photomultiplier. To accomplish this, the light passing through the reference hole in the side of the rotor (at 90° to each of the cell holes) was intercepted by a mirror which reflected the light onto the side window of the stationary RCA 1P28 photomultiplier. Since the position in the image plane corresponding to the reference hole varies with the wavelength of light, delicate alignment problems would be introduced if the mirror–photomultiplier combination were mounted on the absorption optical track. This complication was avoided by mounting this 45° mirror and photomultiplier on the schlieren optical system directly in front of the photographic plate. The stationary photomultiplier thus received a single pulse from the schlieren light source during every revolution of the rotor and the resulting signal was utilized in a switching circuit which automatically could select for examination either of the two double-sector cells. Alternatively the output from the stationary photomultiplier provided the required switching signals when two single-sector cells were being compared.

Although the light reaching the scanning photomultiplier is discontinuous, the final traces produced by the recorder are continuous functions of the optical density of the solutions (relative to the solvents) as a function of position in the cell. Therefore holding circuits are required in order that the reference pulse (in each pair) be stored for comparison with its "mate" (in each pair). Of course the light pulse from each sector must be directed to the correct holding circuit during each revolution of the rotor. Switching within a given pulse pair is achieved as in the earlier version (Lamers *et al.*, 1963) by exploiting the disappearance in light at the trailing end of the reference pulse within each pair of pulses. The trailing edge of each reference pulse activates a one-shot multivibrator which closes the reference gate and automatically opens a sample gate which previously had been closed. In this way the first pulse in any pair is directed to the reference holding circuit and the second to the sample holding circuit. The one-shot multivibrator is particularly effective for this application because it has a built-in recovery time that prevents it from responding to consecutive pulses in a given pair. After this recovery time it reverts to its original form so that the next pulse automatically is fed to the reference holding circuit. Although this characteristic is ideal for discriminating between "mates," the one-shot multivibrator is ineffective in distinguishing between double sector cells separated by 180°. To ensure that a specific pulse pair is routed identically during each revolution of the rotor requires a binary device, known as a flip-flop, which presents a different set of conditions to alternate pulse pairs. The incorporation of this latter unit requires that each pulse pass through two gates, the first operated by the one-shot multivibrator (pair gate) and the second by the flip-flop (cell gate) as seen in Figure 1. Either gate can be in an open or closed position and there are, therefore, four possible states for a given pair of gates. Each gate must be driven by a properly timed signal so that a given set of gates is open only to the single pulse passing at that instant of time. As in the original split-beam scanner the one-shot multivibrator is triggered by the trailing edge of each reference pulse (after some delay and passage through a squaring amplifier). The flip flop in turn is triggered by the trailing edge of each pulse from the one-shot multivibrator. Switching in this manner places no reliance on the sample pulses which are greatly attenuated when solutions of high optical density are being studied. The pair gates operated by the one-shot multivibrator are driven out of phase so that each input pulse passes through only one pair gate, with the first being fed to the reference holding circuit and the second to the sample holding circuit. Selection between the double-sector cells is controlled by the flip-flop. This operates on the cell gates opening them in synchrony so that, for a specific double-sector cell, one cell gate passes the reference pulse and its counterpart passes the "mate." A simple change of the cell selector switch on the console inverts the flip-flop phasing to both cell gates so that they transmit the alternate pulse pairs. In this way two double-sector cells can be examined independently without the need for the prismatic cell windows or wedged cells customarily used for multiple cell operation with either the schlieren or interference optical systems. The synchronizing signal from the stationary photomultiplier (after suitable amplification) is fed directly to the flip-flop so as to ensure that it is in the proper state for the cell under observation, as shown in Figure 1.

When two different samples are to be studied in a single ultracentrifuge experiment, the two double-sector cells are placed in the analytical rotor and the plug normally in the side of the rotor is removed so as to provide a radius mark on all traces. The light passing through this hole when the plug is removed produces the synchronizing signal needed to operate the flip-flop. If only one sample is to be studied, the radius

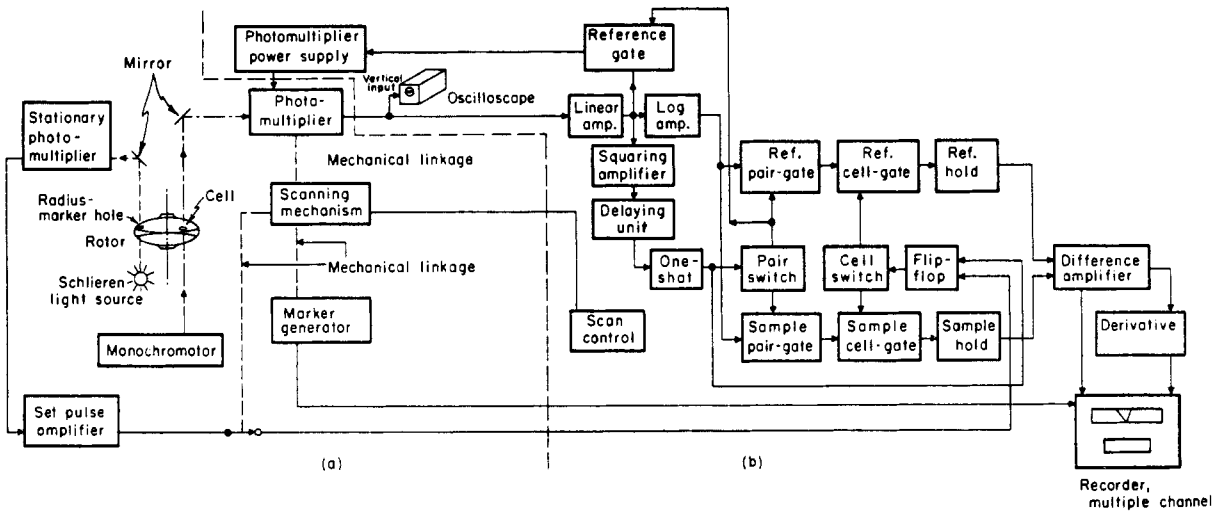

FIGURE 1: Block diagram of the multicell split-beam photoelectric scanner. The section to the left of the dotted line and labeled (a) represents those components which are mounted directly on the ultracentrifuge, and those units to the right of the dotted line labeled (b) correspond to the units which are mounted on the console containing all the electronic controls. The important features for multiplex operation involving either two double-sector cells or two 7° cells mounted 180° apart are shown as (1) the schlieren light source, (2) the radius marker hole, (3) mirror, (4) the stationary photomultiplier, (5) the set pulse amplifier, (6) flip-flop, and (7) the cell switch. For conventional operation, light from the monochromator traverses the cell and, after reflection from the mirror, impinges on the photomultiplier which is operated by the photomultiplier power supply shown in the block diagram. The circuit for regulation of the photomultiplier power supply includes the linear amplifier which is used to amplify all pulses from the photomultiplier, and the reference gate which includes the servomechanism for regulating the photomultiplier power supply. In conventional double-sector cell operation, the signal from the reference cell after passing through the linear amplifier is transmitted to a squaring amplifier and then through a delay circuit to the one-shot multivibrator. This in turn operates the pair switch so that the first pulse after a long dark period is directed through the reference pair gate, and the pulse after the short dark period is directed through the sample pair gate. For multicell operation, an extra switching signal is needed and this is provided by the pulses originating at the stationary photomultiplier which are used to operate the flip-flop mechanism; this in conjunction with a simple switch on the console permits the selection of either of the two cells for observation. In both cases, single cell and multicell operation, the pulses, after being separated, are directed to holding circuits (one for the reference pulse and the second for the sample pulse); from there the two signals are transmitted to a different amplifier where subtraction and amplification is performed. The final result is directly recorded on the multiple-channel recorder. For some purposes, the signals from the difference amplifier are passed through a derivative circuit and then to an independent channel on the recorder. The console also contains the scan control switches permitting automatic selection of the speed of the scanning motor corresponding to periods of 6, 30, 60, and 360 sec. A simple, fast reverse switch also mounted on the console unit permits the rapid return of the photomultiplier to the original starting position. As in the earlier version (Lamers *et al.* 1963), there is a timing marker mounted on the lead screw. This consists of a small accessory light and photosensitive element which in conjunction with the marker generator provides signals for automatic ruling of the recorder paper during each revolution of the lead screw in a given scan. The console contains a series of helipots and switches which permit the recording directly of the transmittance and logarithm of transmittance of either of the two sectors in a double-sector cell. These two types of traces are used in testing the uniformity of illumination of light and focusing the optical system as well as for detecting inadvertent leaks between the two compartments of the cell. The fifth position on the switch is used in routine operation to give traces of the optical density of the solution relative to the solvent. The amplification of the traces can be controlled continuously by means of a helipot and there is a calibrating circuit consisting of a continuously variable electric attenuator which is operated by simple depression of a nulling switch. There is an additional nulling switch which facilitates detecting on the traces the portion corresponding to zero optical density.

marker hole in the rotor is plugged and a counterbalance cell containing two radius marker holes is placed in the second cell hole in the rotor. In addition the circuitry is modified by a switch on the console so that the flip-flop becomes inoperative and both cell gates are open continuously. Synchronizing pulses are unnecessary and the pair gates separate the "mates" as in the earlier design.

The circuitry illustrated schematically in Figure 1 also functions readily for experiments with two single-sector cells one of which contains the solvent and the other the solution. As with two double-sector cells

the plug is removed from the side of the rotor and the light passing through this opening produces a signal on the stationary photomultiplier which triggers the flip-flop. For this mode of operation the pair gates are by-passed, and the pulse separation is controlled by the cell gates. These in turn are operated by the flip-flop which receives one signal/revolution. The solvent and solution cells must be correctly oriented relative to the opening in the side of the rotor so that the first light burst received by the scanning photomultiplier following the synchronizing pulse corresponds to the transmittance of the solvent.

Special precautions were required in the design of the amplifier for the pulses generated by the stationary photomultiplier. Since the AH-6 light source in the schlieren optical system is operated by alternating current, the consequent variation in intensity led to a tenfold fluctuation in the amplitude of the pulse from the stationary photomultiplier. Some compensation for this variation was achieved by the incorporation of the pulse amplifier which raised the low level of the pulses to a satisfactory magnitude while at the same time limiting the high-level pulses. Even with this system, however, spurious triggering occurred on occasion due to scattered light transmitted by the cells themselves. This occurred even though the mirror directing the light to the stationary photomultiplier was positioned so as to avoid the image of the cells and to intercept only the light passing through the reference hole in the rotor. To circumvent this difficulty an adjustable mask was mounted on the schlieren optical track near the schlieren diaphragm (Schachman, 1959). This was placed in such a manner as to intercept the light passing through the cells while light from the radius marker hole passed unattentuated. This mask coupled with the stationary photomultiplier and pulse amplifier produced signals of the quality required for external triggering when the scanner was employed for multiple cell operation.

Linearity. In the earlier version of the split-beam scanning system the limitations in the linearity of the response were caused by the logarithmic compressor used in the circuit. This unit was operated by means of batteries which have been replaced in this modified version by a power supply which has proved to be stable over long periods of time. In addition, special precautions were taken to operate in the proper dynamic range of the logarithmic compressor. This required that the output voltage of the photomultiplier corresponding to the reference pulse be maintained at an optimum level prior to amplification. To achieve this the photomultiplier voltage was adjusted by means of a helipot control to produce 2-v pulses when the scanner received light transmitted by the air space of the reference cell. Occasionally illumination changed across the cell or during the scan of the cell because of fluctuations in light intensity. To counteract the effect of these changes an additional servo system was incorporated. This provided automatic regulation of the photomultiplier voltage so as to maintain a constant output voltage for the reference pulses throughout an entire scan. By means of this feedback regulator the output voltage for the reference pulses was maintained at a constant level and the logarithmic compressor was operated in the optimum dynamic range for maximum linearity.

The photomultiplier power supply was designed to operate in either of two modes: internal or external. When internal regulation was employed the power supply maintained a constant output voltage independent of changes in line voltage or load. This arrangement is ideal for alignment of the optical system so as to obtain uniform illumination across the cell. In external regulation the reference pulses are maintained at a constant amplitude by means of the feedback control which adjusts the power supply voltage to compensate for variations in the output of the photomultiplier. There is an independent reference gate which is used in the servo mechanism and controls the photomultiplier power supply (Figure 1). In the design of this external regulator several difficulties were experienced. When the photomultiplier moved into a dark region of the image the regulator tended to increase the photomultiplier voltage to an excessive value. This extremely high voltage produced noise in the output and, moreover, could lead to damage of the photomultiplier when during a scan it entered an illuminated region of the image. To avoid these regulating problems, additional circuitry was incorporated to limit the maximum voltage produced by the power supply. This ensured that the supply voltage was essentially the same for dark regions as it was when the photomultiplier was receiving high light levels. This was accomplished by the addition of a holding circuit that detected light pulses from the scanning photomultiplier. The voltage from this holding circuit was amplified so as to energize a relay that connects the regulating circuit when light is present. If the light level fell below a prescribed value the relay was deenergized and a dc voltage was substituted for that normally derived from the holding circuit. This voltage is adjustable with a panel control in the console so that the power supply voltage in the absence of light corresponds to that prevailing when the scanner is positioned in an illuminated region. In this way the photomultiplier voltage cannot exceed certain prescribed values and yet control is effected so as to maintain constant photomultiplier outputs even when substantial variations in light intensity occur.

Calibrating Circuit. Since the pulse duration is related directly to the speed of the rotor (as well as the cell angle and the length of the slit at the photomultiplier) and since the capacitors (in the holding circuits) have well-defined time constants the recorder deflection per unit optical density would be expected to be slightly speed dependent. In work heretofore with the split-beam scanning system this speed dependence was observed and the recorder deflection was related to optical density by a series of calibration experiments at specific speeds with solutions of known optical density (Schachman *et al.*, 1962; Lamers *et al.*, 1963). Although this technique worked satisfactorily, it seemed desirable to incorporate into the circuitry an electronic calibrating

device which was independent of speed and would permit the absolute measurement of optical densities. This has been achieved now by incorporating an electrical attenuator which can be varied continuously and calibrated empirically in terms of optical density by comparison with the attenuation caused by solutions of known absorbance. Operation of the calibrating circuit over a long period of time showed its stability and reliability. With this calibrating circuit the optical densities of unknown solutions can be measured directly in an ultracentrifuge experiment by comparing the measured deflections with those produced by the calibrating circuit.

Mechanical Design and Construction. Experience with the first version of the split-beam photoelectric scanner has demonstrated the importance of a four-speed transmission which permitted movement of the photomultiplier slit assembly across the image of the cell at different rates. The emphasis in that work was largely on sedimentation velocity experiments and the scanning times varied from 6 to 36 sec. With slower scanning rates and judicious use of the high-frequency filter on the difference amplifier, it appeared that "noise" could be filtered electronically without a concomitant sacrifice in resolution. Consequently the multispeed transmission was redesigned. The modified four-speed transmission, which operates automatically, employs solenoid-type clutches and permits scanning times of 6, 30, 60, and 360 sec. The solenoids provide remote control of scanning speed and facilitate high-speed return of the scanner regardless of the speed used for the actual recording. The photomultiplier remains at its start position until it receives an impulse from the ultracentrifuge timer after which it moves across the image at a speed controlled by the selection of the solenoid clutch. When the scanner reaches the end of its travel it actuates a limit switch which causes it to return automatically at a fast rate to its start position where it remains until the centrifuge timer provides another impulse. Facilities are incorporated for manual operation as well. At each end of the lead screw an auxiliary set of limit switches is incorporated so as to provide protection for the lead screw in case of malfunction of the principal limit switches.

As in the previous units, a timing generator is incorporated into the scanning unit by mounting on the end of the lead screw a slotted disk which in conjunction with a small light and a photosensitive element generates marker pulses during the revolution of the lead screw. These pulses are fed to two of the galvanometers of the recorder and produce thereby 10 marks during each revolution of the lead screw with every fifth mark being longer than the others. Through this means an automatic check is provided for possible slippage of the two independent drives of the scanner and the recorder. The Visicorder Model 906B is a 14-channel recorder with an extremely fast writing speed which does not limit resolution. Since the Visicorder employs an ultraviolet light beam and photosensitive paper, inking problems are nonexistent and the "pens" can cross one another during the recording. In this way the integral curve and derivative curve can be displayed across the full width of the paper while still retaining a common time base.

Mounted on the front end of the photomultiplier housing is a rotary head which contains six different fixed slits. Three of the slits have lengths of about 2 mm and widths varying from 37 to 150 μ. These short slits were employed with double-sector cells. For those experiments in which the light levels were low and the scanner was to be used with cells separated by 180°, longer slits are placed in front of the photocathode by rotation of the turret containing the six slits. The longer slits (also having widths varying from 37 to 150 μ) were all 10 mm in length corresponding to the diameter of the photocathode. With these longer slits additional light impinged on the photocathode thereby creating a better signal/noise ratio. When high resolution was not required in experiments in which the optical density changed slowly across the cell, wide slits were employed. In most experiments slits of 75 μ width proved adequate.

Derivative Circuits. In the original single-beam system a differentiating circuit was incorporated to produce derivative curves simultaneously with the integral curves (Hanlon *et al.*, 1962). The conversion to a split-beam scanner necessitated a redesign of the derivative circuit and this now has been modified further to include an adjustable filter for reducing high-frequency response and associated noise. In addition a variable gain control has been added along with a positioning control so that the amplitude and position of the trace can be varied readily.

Cell and Optical Alignment. For most experiments conventional double-sector cells with sapphire windows were employed in standard duraluminum or titanium ultracentrifuge rotors. The window holders contained a central rib, and the two openings in both the lower and upper window holders were rectangular in shape with the openings being slightly narrower than the sectorial cavities of the centerpiece. For those experiments involving the far-ultraviolet region of the spectrum (where light levels were low) special single-sector cells were used. These had 7° sector angles and were produced by removal of the rib in conventional double-sector centerpieces. In addition the central rib in the window holders was removed. In some sedimentation equilibrium studies three samples were analyzed in a single experiment through the use of the multicompartment, double-channel cell described by Yphantis (1964).

Conventional single-sector counterbalances were employed for most of the work. These provided in each trace the data necessary for determining the magnification of the optical system as well as providing known references for distances from the axis of rotation. When the scanner was used in conjunction with the Rayleigh interference optical system the single-sector counterbalances were modified by enlargement of the holes in the counterbalance so that the width of the opening was sufficiently large to permit the formation of interference fringes in the images of the

reference holes. In some experiments a special counterbalance cell of different design was employed. This contained two sets of rectangular openings at positions corresponding to those generally used in counterbalances for the interference optical system. One set of rectangular openings was of a slightly longer dimension (in a radial direction) than the other. When the scanner traversed the region of the image corresponding to the one opening a trace corresponding to infinite optical density was produced; as the scanner moved across the image it came to the region in which the two conjugate rectangular openings traversed the optical path thereby leading to zero optical density. This latter region was of considerable use in nulling the instrument for zero optical density. Without such a cell the nulling procedure described previously was employed. This utilized a region of the image in the air space above the solvent and solution columns where the transmittance was the same in both halves of the double-sector cell. Finding such a region in the cell was often difficult since the windows above the liquid column frequently transmitted light to varying extents due to the differential wetting of the windows by the liquids of unequal optical densities.

The procedure described earlier for alignment of the optical system was used throughout (Schachman *et al.*, 1962). A substantial increase in light level was achieved by substituting for the General Electric H85A3 light source a high-pressure mercury xenon arc lamp manufactured by PEK Laboratories, Palo Alto, Calif. This 100-w source is powered by a dc supply producing a current of about 5 amp and a voltage of 20 v. Through the kind cooperation of L. Gropper, Spinco Division of Beckman Instruments, Inc., a modified back plate was constructed for use with the DU monochromator. This permitted controlled positioning of the lamp in the housing as well as adjustment of the two mirrors needed to focus the source onto the entrance slit of the monochromator. Early experience with this source indicated that the light levels in the far-ultraviolet could be enhanced substantially by blowing an air stream onto the lamp and thereby decreasing its operating temperature slightly. Accordingly, a fan motor with controlled inlet and outlet vents was incorporated onto the left side of the light-source housing and the cooling fan was used for those experiments involving wavelengths below 280 mμ. A newer version of the back plate and light-source housing assembly has mounted onto it a cooling fan which permits the needed control of the temperature of the light source for work in the far-ultraviolet region of the spectrum.

The monochromator was aligned according to the manufacturer's specifications and its position was adjusted in accordance with the procedure described earlier (Schachman *et al.*, 1962). In order to reduce problems arising from stray light, masks were mounted on the collimating and condensing lenses. These two masks contained adjustable rectangular openings about 4 mm in width and 20 mm in length. Care was taken to ensure that the openings were parallel to a radius through the center of the drive unit. Alignment of the lower mask was performed by examining the image with visible light when the rotor was mounted on the drive unit and fixed in a stationary position. The upper mask was oriented relative to the lower mask by examining the light pattern impinging on the upper mask after the lower one had been positioned correctly. These two apertures helped to reduce reflections and scattering from the lenses without impairing the light level needed for satisfactory operation of the scanner. In addition to these masks a third mask was mounted at the position of the 45° mirror at the top of the optical track. This had a small, rectangular opening just large enough to allow the principal image to pass through it while at the same time intercepting some of the stray light that would otherwise be focused by the camera lens onto the image of the rotating cell. Elimination of this stray light had a marked effect in increasing the linearity of the response of the recorder as a function of optical density. Without these limiting apertures in the vacuum chamber, the image of the reference cell was "seen" by the photomultiplier even after it had passed the optical axis of the system and the solution cell was centered in the optical path. As a consequence with solutions of high optical density, the stray light which appeared in the image of the sample cell led to apparent optical densities less than the true values; therefore, elimination of this stray light is especially important.

Materials and Methods

Chromatographically purified bovine plasma albumin[1] was kindly provided by R. W. Hartley and H. A. Sober. Rabbit muscle aldolase was prepared according to the method of Taylor *et al.* (1948) and recrystallized twice from ammonium sulfate. Ribonuclease A (chromatographically prepared) was obtained from the Worthington Corp., Lot No. RAS 6018. Human hemoglobin was kindly furnished by L. Stryer. Myoglobin (sperm whale) was obtained from Mann Research Laboratory, Lot No. K 1387. Aspartate transcarbamylase was kindly provided by J. C. Gerhart. Adenosine and *dl*-tryptophan were obtained from Nutritional Biochemicals Corp., and maleic acid from Matheson Coleman and Bell. The procedure of Bessman *et al.* (1958) was used for the synthesis of 5-bromocytidine triphosphate.

Protein concentrations were evaluated from absorbance measurements with a Zeiss PMQII spectrophotometer. The following extinction coefficients, $\epsilon_{1cm}^{0.1\%}$ at 280 mμ, were employed: BPA, 0.667; aldolase, 0.91; ribonuclease, 0.695; ATCase, 0.59. For hemoglobin and myoglobin the analogous extinction coefficients at 410 mμ were taken as 8.4 and 9.0, respectively. Adenosine concentrations were estimated from $\epsilon_{1cm}^{0.1\%} = 55$ at 260 mμ.

Double-sector cells (aluminum filled epon) were employed in most experiments with solvent in one compartment (the right-hand side with the screw ring facing forward) and the sample solution in the other. For experiments with light of low wavelength (λ 230

mμ) the center rib of the double sector cell was removed by careful milling and the resulting 7° single-sector centerpieces were used with special window holders the openings of which were enlarged so that light could traverse the entire cross section of the liquid column. These cells were used in pairs, one containing the solvent and the other the solution, and the windows were selected for equal transmittances. Sapphire windows were employed for most experiments although some of the older windows were found to absorb appreciable amounts of light at wavelengths below 250 mμ.

For many sedimentation equilibrium studies both Rayleigh interference patterns and scanner patterns were obtained in a single experiment. To accomplish this wide window holders were employed in the ultracentrifuge cells (a requirement of the photoelectric scanner). The interference patterns were produced through the use of a narrow Rayleigh mask mounted on the condensing lens of the vacuum chamber (Richards and Schachman, 1959). Experiments were designed to be either high speed, as described by Yphantis (1964) so as to give virtually zero solute concentration at the meniscus, or low speed (Richards and Schachman, 1959) which yielded finite solute concentrations throughout the liquid column. For the latter experiments the fringe number was determined according to the method of LaBar (1965) by overspeeding the rotor after equilibrium was attained. Column heights of 3 mm were employed routinely; only in some experiments with adenosine were longer liquid columns used. The apparent weight-average molecular weights were calculated from plots of the logarithm of the recorder deflection (or fringe number or displacement) *vs.* the square of the distance (in centimeters) from the axis of rotation. In calculations of the molecular weight the following values of the partial specific volume (milliliters per gram) were employed: BPA, 0.734 (Dayhoff *et al.*, 1952); aldolase, 0.742 (Taylor and Lowry, 1956); ribonuclease, 0.695 (Harrington and Schellman, 1956); ATCase, 0.74 (assumed); hemoglobin, 0.749 (Svedberg and Pedersen, 1940); myoglobin, 0.741 (Theorell, 1934); and adenosine, 0.638 (Hanlon *et al.*, 1962).

Since most of the sedimentation equilibrium experiments involved solutions of extremely low concentrations special precautions were exercised to minimize possible convective disturbances. All solutions contained relatively high concentrations of salt ions in order to produce appreciable density gradients due to the redistribution of the buffer constituents. Speeds were as high as possible consistent with the nature of the solute molecules and the desired concentration distribution. The heater normally operated by signals from the thermister mounted in the base of the ultracentrifuge rotor was not used. Instead the temperature was controlled by the refrigeration unit which was adjusted to produce rotor temperatures of 5–17°. Although a predetermined temperature could not be attained precisely because of the lack of sensitivity of the refrigeration control, the temperature was maintained constant at the end of each experiment (as indicated by the resistance measured with the rotor temperature indicator and control).

An indirect method was employed for the determination of the magnification of the absorption optical system. A single-sector cell was fillled with 0.1 ml of CCl_4 and 0.2 ml of H_2O and both schlieren patterns and scanner tracings were obtained with the rotor spinning at about 20,000 rpm. The distance between the air–H_2O interface and the H_2O–CCl_4 interface was measured on both patterns and the ratio obtained for different wavelengths. From these ratios and the known value of the magnification of the schlieren optical system (as measured with a ruled glass disc in a stationary rotor) the distances on the recorder traces were correlated directly with distances in the rotating ultracentrifuge cell. Focusing the camera lens of the absorption optical system for different wavelengths was performed through the use of off-axis illumination as described earlier (Schachman *et al.*, 1962).

Performance of Multicell Photoelectric Scanner

Multicell Operations. Figure 2 shows the pulses generated at the photomultiplier when two double-sector cells were used in one experiment and the radius marker hole in the rotor was employed to produce switching pulses at the stationary photomultiplier mounted on the schlieren optical track. The oscilloscope traces illustrate the amplitude, duration, and separation of the light bursts at different places in the images of the ultracentrifuge cells. Since the time scale of the oscilloscope trace was adjusted (relative to the rotor speed) to portray more than one revolution of the rotor, the pulses from the separate compartments of each double-sector cell were extremely close and only barely distinguishable in some of the traces. For the upper pattern, Figure 2a, the photomultiplier was positioned to record the light transmitted by the air spaces above the four liquid columns. Consequently the pulse heights were equal. The first pair represents cell 1 and the next pair, corresponding to one-half revolution of the rotor, shows the pulses caused by cell 2. The third double pulse represents cell 1 after a complete revolution of the rotor. Beneath this trace is one showing the pulse produced by the stationary photomultiplier. Only one light burst strikes this photomultiplier in a complete revolution of the rotor since the hole in the opposite side of the rotor is blocked by a counterweight. The occurrence of the double pulses from cells 1 and 2 relative to the switching pulse from the stationary photomultiplier is illustrated clearly in the oscilloscope pattern.

When the photomultiplier-slit assembly was moved along the image (in a centrifugal direction) the intensity of light striking the photocathode provided a measure of the transmittances of the liquids in the cells. In Figure 2b are the oscilloscope traces when the reference compartments in each double-sector cell were filled with water and the sample compartments contained solutions of tryptophan of different concentrations. The second pulse of the first pair (cell 1) was significantly greater than that corresponding to the solution

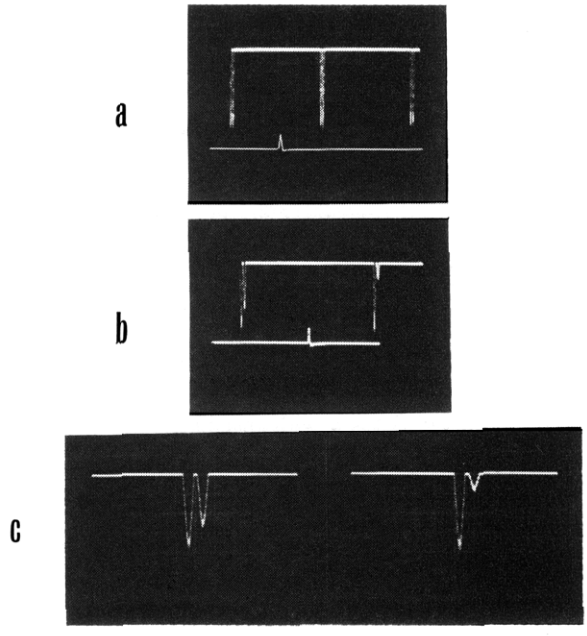

FIGURE 2: Oscilloscope traces illustrating photomultiplier pulses observed with two double-sector cells. For each cell the reference compartment contained distilled water and the sample compartments were filled with tryptophan solutions having optical densities of 0.15 and 0.625, respectively. (a) The scanner was positioned to intercept the images of the air spaces above the liquid columns in the four sectors. The upper pulses (with increasing intensity pointing downward) correspond to light striking the scanning photomultiplier. The lower pulse (pointing upward) represents the light striking the stationary photomultiplier mounted on the schlieren optical system. This light passes through the radius marker hole in the side of the rotor and the signal from the photomultiplier is utilized to operate the flip-flop used in the switching circuit to differentiate the two cells. The time scale for the oscilloscope patterns is such as to represent slightly more than one revolution of the rotor, and therefore only one light pulse from the stationary photomultiplier is observed and three double pulses impinge on the scanning photomultiplier. (b) The photomultiplier was moved along the image so as to intercept light transmitted by the liquid columns in the four compartments of the two double-sector cells. Cell 1 contains the solution with OD 0.15 and cell 2 contains the solution with OD 0.625. The time scale was adjusted so that only slightly more than one-half revolution of the rotor is illustrated. The pulse to the stationary photomultiplier is illustrated below. (c) The conditions were the same as in (b) except that the time scale for the oscilloscope patterns was adjusted in order to expand the pulses for each sector and thereby to facilitate visualization of the dark period between reference and sample compartments. The pulse from the stationary photomultiplier is not shown.

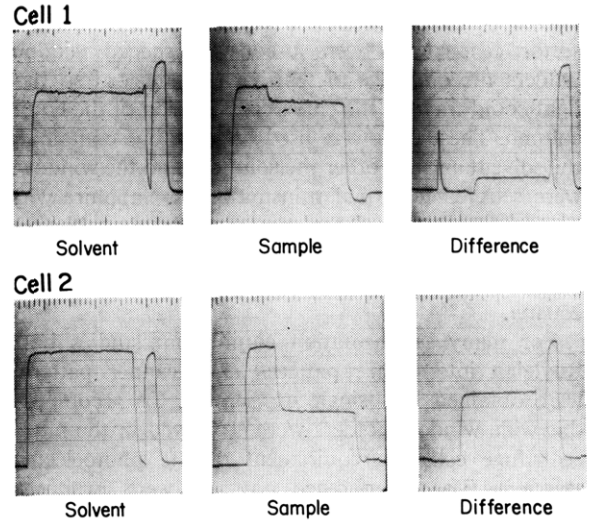

FIGURE 3: Recorder traces illustrating performance with two double-sector cells. These traces were obtained in the experiment represented by Figure 2 showing the various modes of operation of the photoelectric scanner. At the top are shown the patterns for cell 1 and beneath them are the analogous patterns for cell 2. All traces represent signals passing through the logarithmic compressor. On the left are the diagrams for the reference (solvent sector) with increasing intensity of light in the vertical direction. The center patterns represent the logarithm of the transmittance of the sample compartments with the intensity of the transmitted light increasing in the vertical direction. On the right are the patterns obtained when the mode is switched to split-beam operation and they represent the optical density *vs.* distance for the solution relative to the solvent. For these traces the optical density increases in a vertical direction. In all traces increasing distance from the axis of rotation is to the right.

in cell 2. For these oscilloscope patterns the time scale was adjusted to represent slightly more than one-half revolution of the rotor. The pulse from the stationary photomultiplier, as in Figure 2a, occurred (in terms of time) after the pulses from cell 1 and prior to cell 2. In the next one-half turn of the rotor there would not be a pulse from the stationary photomultiplier. To illustrate the differences in the transmittances of the two tryptophan solutions (relative to water) the time scale was expanded still further in Figure 2c.

The recording of the optical densities of the two solutions relative to the solvent requires the separation of the four light pulses, conversion of the intensities to their logarithmic values, subtracting the second in each pulse pair from the first, and plotting the difference after suitable amplification. This is performed continuously as the photomultiplier-slit assembly traverses the image slowly (relative to the speed of the appearance of light bursts). In this way a continuous curve is constructed representing the corrected optical

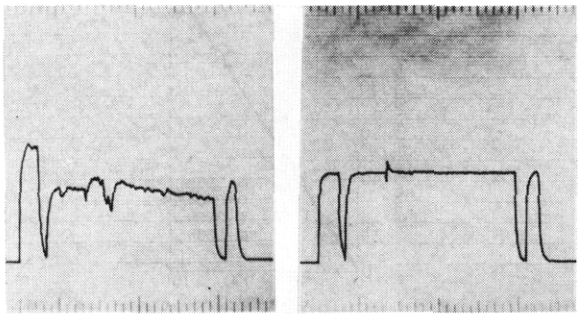

FIGURE 4: Recorder traces illustrating feedback regulation of the photomultiplier voltage. One double-sector cell was used in this experiment and the reference compartment was filled with distilled water. On the left is the trace of the intensity of light transmitted through the reference cell. Considerable noise was observed and the illumination was nonuniform due to accumulated dust and oil on the lenses of the vacuum chamber. This is a pattern observed when the photomultiplier voltage is maintained at a constant level controlled by the setting of a helipot on the power supply. When the feedback circuit is incorporated the pattern on the right was observed. In this mode of operation nonuniform illumination as well as fluctuations in light intensity are automatically corrected by having the signal reaching the photomultiplier through the reference cell fed back in a servo control and thereby adjusting the photomultiplier voltage automatically during the scan of the image.

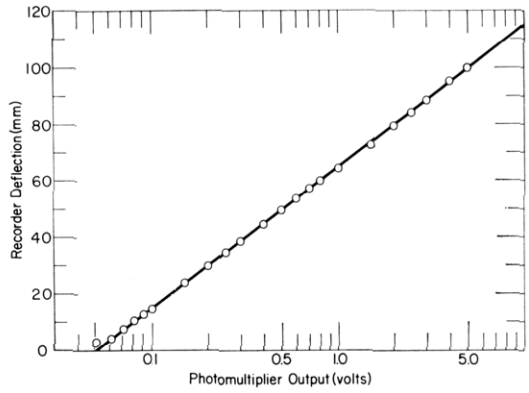

FIGURE 5: Performance of the logarithmic compressor. The ordinate represents the recorder deflection in millimeters and the abscissa the photomultiplier output in volts (on a logarithmic scale). The photomultiplier slit assembly was moved along the image so as to intercept light transmitted by the radius marker hole in the counterbalance and the photomultiplier supply voltage was adjusted manually to produce light pulses of various magnitudes. The size of these pulses was measured on an oscilloscope and the signals were correspondingly produced on the visicorder traces as the logarithm of the light intensity. For this experiment the switching circuits were disabled and in this way the logarithmic compressor was tested directly in terms of its input and output.

density of each solution as a function of distance from the axis of rotation. The patterns produced by the scanner are given in Figure 3. At the top are shown the patterns for cell 1 and below are the analogous patterns for cell 2. Only the logarithmic traces are illustrated; on the left are curves for the reference (solvent) compartment, in the center are the sample (solution) traces, and the right-hand traces represent the automatically subtracted traces (split-beam operation).

Figure 3 shows that two samples can be analyzed in a single experiment. The results obtained in this way are indistinguishable from those produced in two separate experiments with individual double-sector cells. Thus, through multicell operation a considerable saving in time can be effected without a sacrifice in accuracy. This is particularly useful in testing the linearity of the complete optical system since several samples can be examined at the same time. With multicompartment double-channel cells (Yphantis, 1964) six different solutions can be examined in a single experiment. Multicell operation is particularly useful for sedimentation equilibrium studies requiring overnight centrifuge experiments.

Feedback Regulation of Photomultiplier Output. After continuous use of the high-intensity light sources in the monochromator for periods of several hundred hours, fluctuations in light intensity become prevalent and frequently the intensity during a scan fell too low to sustain the switching level. In addition, the optimum dynamic range of the logarithmic convertor was not utilized since the reference pulses often were below the desired 2-v level. Both of these difficulties were readily circumvented through the use of the servo mechanism which adjusted automatically the voltage applied to the photomultiplier so as to maintain a constant output. The performance of this feedback regulator circuit is illustrated by the patterns in Figure 4 which represent the intensity of the light transmitted by the reference cell containing water. It should be noted that the logarithmic compressor was by-passed for this experiment so as to see more clearly the changes in light intensity. On the left is the trace produced when a constant photomultiplier voltage is applied. Not only was the light intensity fluctuating during the period of the scan, but also the illumination across the cell was not uniform. This is detected by comparing the heights of the traces corresponding to the images of the reference holes in the counterbalance cell. When the feedback regulation was applied the trace became exceedingly smooth as seen in the right-hand trace of Figure 4; moreover the nonuniform illumination was compensated for automatically.

The feedback regulation of the photomultiplier voltage is also very useful in correcting for nonuniformity in illumination due to scattering from oil and dust deposits on the collimating and condensing lenses. It is valuable also for ultracentrifuge experiments in

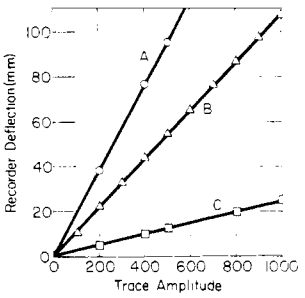

FIGURE 6: Performance of the amplification of the recording system. The recorder deflection in millimeters is plotted on the ordinate as a function of the trace amplitude on the abscissa. The units for the trace amplitude represent the divisions of the helipot with 1000 corresponding to maximum gain. Three different experiments were performed in each of which the reference compartment was filled with distilled water and the solution compartments with tryptophan solutions of different optical densities. The rotor speed was about 24,000 rpm and the wavelength on the monochromator was 280 mμ with a slit opening in the monochromator of 2 mm. Curve A represents a solution having an optical density of 0.95, B corresponds to 0.54, and C to 0.125.

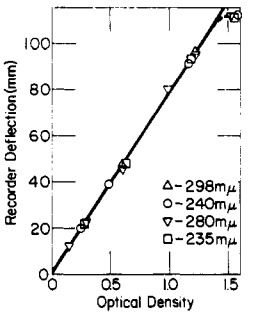

FIGURE 7: Linearity of the recording system as a function of optical density. Solutions of known optical density were examined at various wavelengths in a double-sector cell with distilled water as the reference liquid. The recorder deflection in millimeters is plotted on the ordinate as a function of optical density on the abscissa. All optical densities for the solutions were measured in a Zeiss spectrophotometer and converted to a thickness of 12 mm to correspond to the optical path of the ultracentrifuge cells. All measurements were made at a trace amplitude of 500 and the rotor speed was 59,780 rpm. Measurements were made with solutions of tryptophan at 280 mμ ▽; BrCTP at 298 mμ △; and maleate at 235 mμ □ and 240 mμ ○.

which light of low wavelength (about 230 mμ) is employed. Under these circumstances buffer ions or components like mercaptoethanol absorb so much of the incident light that the split-beam system cannot function effectively without continuous adjustment of the photomultiplier voltage. A similar complication occurs in experiments involving a sedimenting component in each compartment (Richards and Schachman, 1957, 1959; Schachman, 1963a). All of these difficulties are obviated by the incorporation of the photomultiplier regulating circuit since the output from the reference cell is maintained at a constant value throughout the scan.

Linearity of Electronic Circuits. Assessing the linearity of the response of the recording system to variations in optical density required tests of the performance of each of the critical components in the photoelectric scanner. One of these is the logarithmic compressor which converts the output of the photomultiplier into the logarithmic value required for recording the results in terms of optical densities. To test this unit, the output of the photomultiplier in volts was varied by discrete amounts and measured directly on the oscilloscope (see legend to Figure 5 for details of the procedure). Simultaneously the logarithm of the output of the reference holding circuit was measured directly from the galvanometer deflection of the recorder. As seen in Figure 5 the response was linear. The range of measurements covered a range of photomultiplier voltages varying from 5 to 0.05 v corresponding to an effective optical density of 2. Except for the switching circuit which was disabled deliberately to prevent spurious switching spikes when the photomultiplier output was very low (2 v is the normal operating voltage) this test involved the complete electronic system from photomultiplier to recorder.

In many sedimentation velocity studies, especially with mixtures of components, the gain on the amplifier is altered during the experiment in order to measure the amounts of the different molecular species. As a consequence it was necessary to test the linearity of the recording system as a function of the trace amplitude. For the data presented in Figure 6, three experiments were performed with different solutions of tryptophan varying in optical density from 0.125 to 0.95. In each experiment the response was measured directly in millimeters on the recorder traces made at different amplifications. The results in Figure 6 show that the recorder deflection is directly proportional to the trace amplitude. Figure 6 also provides an indication of the sensitivity of the scanner. A solution having an optical density of 0.125 produced a deflection of 25 mm with full gain on the amplifier. Since deflections of 2–4 mm are ample for certain types of sedimentation experiments, successful studies can be conducted with solutions having optical densities of only about 0.02.

Linearity of Recorder Response to Variations in Concentration and Measurement of Extinction Coefficients. Since the experiments described above indicated that the logarithmic compressor, holding circuit, amplifiers, and recorder functioned satisfactorily, the performance of the entire optical system was tested in two types of experiments. In the first of these the double-sector cell was filled with solvent (water) in the reference

compartment and a series of solutions (in succession) of varying concentrations (or optical densities) were placed in the sample compartment. For these experiments the centrifugal field was sufficiently low, in terms of the molecular weight of the solute, that the optical density was uniform throughout the cell.

Figure 7 shows the data from a series of experiments with tryptophan, BrCTP, and maleate. Direct proportionality was obtained between recorder deflection and optical density (measured independently in a spectrophotometer). Identical results were observed at a variety of wavelengths with the slope of the line depending on the gain on the amplifier (see Figure 6). With solutions having optical densities greater than about 1.2 the response of the recording system was no longer proportional to the concentration of the solute. Since this deviation from linear behavior could not be attributed to malfunctioning of the electronic components of the scanning system, the limitations must have arisen from optical problems such as stray light. The removal of the light-limiting apertures mounted on the collimating and condensing lenses decreased the range of linearity of the recorder response. This indicated that the departure from linearity for the highly absorbing solutions resulted from stray light appearing in the image of the solution compartment as it passed by the photomultiplier-slit assembly. This represents one of the principal difficulties with the split-beam scanning system. If no limiting masks are placed in the vacuum chamber (near the rotor) the two compartments of the double-sector cell are illuminated and imaged simultaneously by the camera lens at the slit just in front of the photocathode of the photomultiplier. This occurs even though the images move across the focal plane. As a consequence of imperfections in the focusing process, due, for example, to scattering of light from oil and dust deposits on the lenses, the images of the two individual compartments overlap partially. To prevent this, the two limiting apertures were placed on the lenses of the vacuum chamber. In this way, at any instant only one cell compartment is illuminated and only it is "seen" by the photomultiplier. The effect of stray light was thereby minimized and the range of linear response enhanced.

The data presented in Figure 7 cannot be taken as an absolute calibration of the recording system in terms of optical densities since the response varied slightly with rotor speed. This speed dependence is reduced somewhat by selecting holding capacitors of different sizes (and time constants) for various rotor speeds. In addition the electric attenuator (calibrating circuit) when used in conjunction with data like that in Figure 7 provides an absolute measurement of the optical density which is not affected by rotor speed. Thus absolute optical densities can be measured directly from the recordings.

The linearity of the recording system was tested independently in another manner. This involved only a single experiment and the combined use of the photoelectric scanner and the Rayleigh interference optical system. By judicious selection of the rotor speed in terms of the molecular weight of the solute an appreciable concentration gradient was produced under the influence of the centrifugal field. This concentration distribution as a function of position in the cell was measured with the interference optical system, and the photoelectric scanner was employed to obtain a curve of recorder deflection *vs.* distance. Cross-plotting of the data at corresponding positions gave directly the relationship between recorder deflection (or optical density) and fringe displacement (or solute concentration). Bovine plasma albumin, because of its relatively low extinction coefficient per unit weight and large molecular weight, proved an ideal substance for examination simultaneously by interference optics and the scanner (with light having a wavelength of 280 mμ). Figure 8 presents the data from a sedimentation equilibrium experiment with this protein. The speed was sufficiently high that the protein concentration at equilibrium was virtually zero at the meniscus. As seen in Figure 8 the recorder deflection was directly proportional to the fringe displacement (or solute concentration). This result is in excellent agreement with those shown in Figure 7 demonstrating the linearity of the response of the recording system to variations in optical density. Moreover, the demonstrated linearity in the sedimentation equilibrium experiment shows that stray light directed in a radial direction (from a region of low optical density to one of high absorbance) must be negligibly small in magnitude. Otherwise the observed (or apparent) optical density at the bottom of the cell would be less than the true value.

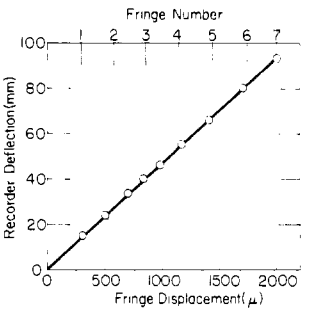

FIGURE 8: Linearity test by combined use of interference optics and photoelectric scanner. The ordinate represents the recorder deflection in millimeters and the abscissa the fringe displacement in microns on the lower scale and as fringe number on the upper scale. The data were obtained from a sedimentation equilibrium experiment on bovine plasma albumin, at an initial concentration of 0.6 mg/ml in 0.1 M NaCl–0.01 M acetate buffer, pH 5.4. The rotor speed was 24,630 rpm. To obtain the data for this graph the recorder deflections and the fringe displacements were measured at corresponding values of the distance from the axis of rotation and then cross-plotted to produce the results shown above.

The values of the recorder deflections shown in Figure 8 can be transposed into optical densities from

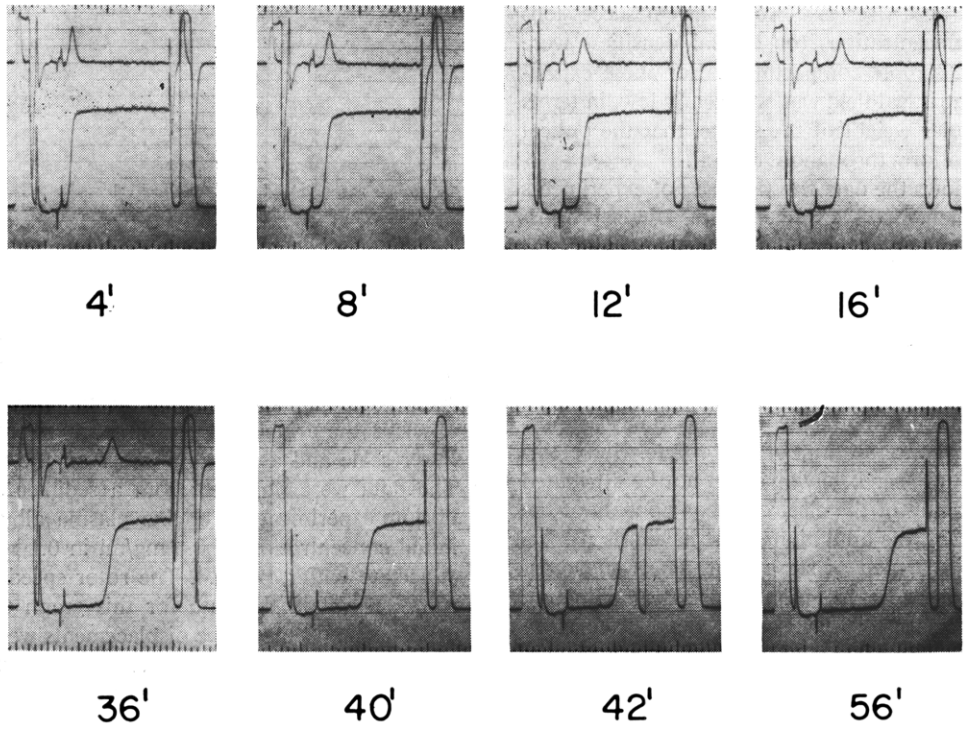

FIGURE 9: Sedimentation velocity patterns of aspartate transcarbamylase. The times after attaining a speed of 50,740 rpm were shown below each pattern. Sedimentation is to the right and increasing concentration (optical density) is in the upward direction. The optical density at 280 mμ (in a 1-cm cell) was 0.9 and the slit width on the monochromator of the ultracentrifuge was 2 mm. The two small vertical spikes at the base line correspond to the menisci of the solvent (pointing in a negative direction) and the solution (in the positive direction). The traces at the left and right of each pattern represent light passing through the inner and outer reference holes of the counterbalance cell. The horizontal grid lines with each fifth line (representing spacings of 10 mm) being slightly heavier than the others are ruled automatically by the recorder as the trace is produced. The vertical lines at the top and bottom of each pattern are drawn by two of the recording galvanometers which receive impulses from the timing generator. The timing marks provide an unambiguous measure of the movement of the photomultiplier in terms of the fractional rotation of the lead screw. In five of the patterns both the integral and derivative traces are shown, being produced by the recording system simultaneously. After the 36-min picture was obtained the derivative pattern was turned off-scale so that the traces corresponding to the reference holes could be seen more clearly. In the 42-min trace after the photomultiplier had moved into the image of the plateau region of the cell the null switch on the console was depressed to show the actual base line corresponding to zero optical density. It should be noted that this null position actually is at a level slightly below that corresponding to the supernatant region. This shows that the supernatant liquid in the solution compartment absorbs a small amount of light presumably due to some mercaptoethanol in the buffer that was not duplicated in the reference compartment. For all of these traces the scanning time was 30 sec and the trace amplitude was set at 400. The buffer was 0.1 M Tris–HCl at pH 8 containing 10^{-3} M mercaptoethanol and 10^{-4} M EDTA.

the calibration curves of Figure 6 and Figure 7. Similarly the fringe displacement (or fringe number) is readily converted to refractive index difference or solute concentration (Richards and Schachman, 1959; Schachman, 1963b). Thus a combination of these factors coupled with the data of Figure 8 gives directly the extinction coefficient of the sedimenting substance. With the known refractive increment, 0.0019 dl/g, for bovine plasma albumin (Perlmann and Longsworth, 1948), the cell thickness, 11.92 mm, and the wavelength of the light employed in the Rayleigh optical system, 5460 A, the number of fringes expected for a 1% solution is calculated to be 41.5. Generally the number of fringes observed is slightly less (about 40) than the calculated value (E. G. Richards and H. K. Schachman, in preparation). Apparently the effective wavelength of the light responsible for the interference fringes is slightly greater than that normally transmitted by the filter in the optical system, and 40 fringes is taken as the number of fringes expected for a 1% solution of bovine plasma albumin. When this number is combined with the slope of the line in Figure 8 and the calibration data of Figure 7, an extinction coefficient ($\epsilon_{1\text{ cm}}^{0.1\%}$) of 0.68 is obtained for light having a wave length of 280 mμ. This is in excellent agreement with the value 0.67 measured from spectrophotometry of solutions

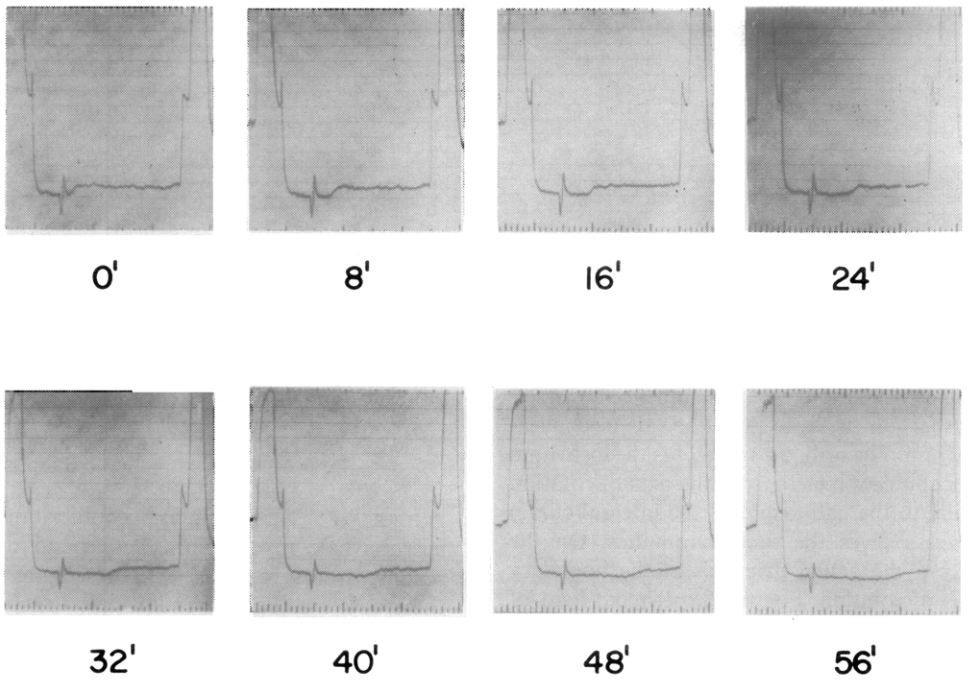

FIGURE 10: Sedimentation velocity patterns of a dilute solution of aspartate transcarbamylase. For this experiment the protein concentration was 20 μg/ml and the wavelength of light was 235 mμ. In all other respects the experimental conditions were similar to those described in the legend to Figure 9.

of known concentration (Hartley *et al.*, 1962).

These experiments involving all of the optical and electronic components of the scanning system show clearly that the recorder response is directly proportional to the optical density of the solution in the ultracentrifuge cell. Moreover, absolute concentrations can be measured accurately and conveniently from the recorder deflection.

Sedimentation Velocity Studies

Figure 9 shows a series of patterns from a sedimentation velocity experiment on ATCase. This enzyme has a relatively low extinction coefficient at 280 mμ, $\epsilon_{1cm}^{1\%}$ 5.9 (Gerhart and Schachman, 1965), and the concentration, 0.15%, in this experiment was only slightly lower than that customarily employed for ultracentrifuge studies with schlieren optics. However, the photoelectric scanner was used at comparatively low amplification and the sensitivity is such that the concentration could be reduced 20-fold and the recorder deflection would still be sufficiently large as to permit accurate measurements of the boundary positions. An intermediate scanning rate (30 sec for the complete scan of the image) was employed for the traces in Figure 9, and the electronic filter was adjusted to minimize photomultiplier "noise." In this way comparatively noise-free traces were obtained without sacrificing resolution in the radial direction. This is illustrated by the sharp images of the menisci in the two compartments of the cell. Despite the slow scanning rate the derivative patterns were of high quality, permitting accurate measurements of boundary positions and shapes. The quality of the derivative patterns is enhanced by scanning at a faster rate (a 6-sec scanning period). During the scan represented by the 42-min pattern the null (or base line) switch on the console was depressed when the photomultiplier-slit assembly was in a region of the image corresponding to high optical density. This nulling procedure disconnects the input pulses, thereby causing the recorder trace to indicate the position representing zero optical density. It should be noted that depressing the null switch caused the trace to fall to a value equal to that in the air space above the two liquid columns since the transmittance there was the scan for both compartments. However, in the supernatant region behind the ATCase boundary the optical density was not zero. This optical density (about 0.03) was due to mercaptoethanol in the enzyme solution (which was not present in the buffer placed in the solvent compartment).

Extremely dilute solutions of proteins can be studied readily by using light of lower wavelength as seen in Figure 10. For these traces the amplification of the recording system was increased to its maximum value and the wavelength of the incident light was reduced to 235 mμ so as to exploit the absorption due to the peptide bonds. The boundary position is readily determined from the traces even though the optical density of the solution was only about 0.03 (corresponding to a protein concentration of 20 μg/ml). For studies of even more dilute solutions the solvent and solution were placed in separate 7° cells and a longer slit (10 mm) was used in the photomultiplier-slit assembly.

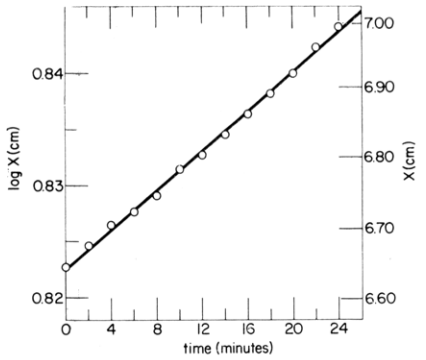

FIGURE 11: Determination of the sedimentation coefficient of aspartate transcarbamylase at a concentration of 3 μg/ml. The ordinate represents the logarithm of the distance in centimeters from the axis of rotation (corresponding to the half-height of the integral curve) and the abscissa gives the time in minutes. On the right are shown the actual distances of the boundary from the axis of rotation. For this experiment light of 230 mμ was used, the solvent and solution were placed in separate 7° cells, and the slit used in front of the photomultiplier was 10 mm in length. The operating speed was 59,780 rpm and traces were recorded at 2-min intervals. The buffer was 0.1 M phosphate at pH 7 containing 10^{-4} M EDTA.

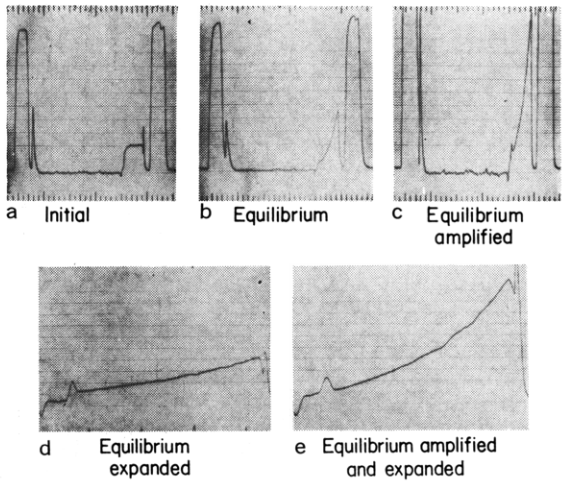

FIGURE 12: Sedimentation equilibrium patterns of sperm whale myoglobin. The general description of scanner traces in the legend of Figure 9 applies to these patterns. The upper left pattern was recorded at zero time, while the remaining equilibrium patterns were obtained after 18 hr of centrifugation at a speed of 31,410 rpm. The upper center pattern was recorded at a low trace amplitude (400), selected to contain the deflections of the reference holes within the trace. The upper right pattern was recorded at the maximum trace amplitude (1000). The three upper patterns were recorded with a scan time of 30 sec with the recorder paper moving at 5 mm/sec. The lower patterns were produced with a scan time of 6 min with the chart speed the same as above, although only the solution column was recorded. The left and right lower patterns were obtained at trace amplitudes of 400 and 1000, respectively. The traces were recorded with light of 405 mμ. The solvent was 0.1 M phosphate buffer at pH 7.0 and the initial protein concentration was 0.025 mg/ml.

By this means light of even shorter wavelength could be employed satisfactorily without the need for excessively high photomultiplier voltages. Satisfactory traces were obtained with light of wavelength slightly below 230 mμ, and absorption due to the buffer ions introduced no complications since the split-beam operation corrected automatically for this effect. As seen in Figure 11 accurate sedimentation coefficients can be determined with solutions having a concentration of only 3 μg/ml. It is important to note that the value, 11.7 S, for ATCase corresponds to that expected from studies at higher concentrations, thereby showing that ATCase does not dissociate into subunits upon dilution in a buffer at pH 7. The range of concentrations can be extended still further through the use of cells with longer optical path (30 instead of 12 mm). Thus through the use of light with a wavelength of about 230 mμ sedimentation coefficients can be measured routinely at concentrations of 1 μg/ml. This should be particularly useful in studies of interacting systems involving association–dissociation equilibria.

Sedimentation Equilibrium Studies

Figure 12 illustrates various scanner patterns obtained in sedimentation equilibrium experiments. On the left is the pattern observed shortly after the rotor attained the desired speed in an experiment with myoglobin. Since myoglobin possesses such a high extinction coefficient at 405 mμ the initial concentration was only 0.0025 g/100 ml. In order to reduce the time required to reach sedimentation equilibrium only 0.1 ml of solution was placed in the sample compartment of the double-sector cell and 0.11 ml of solvent was added to the reference compartment (Van Holde and Baldwin, 1958). Most of the trace shows, therefore, zero optical density corresponding to the air spaces above the two liquid columns. The pattern observed at equilibrium (18 hr) is shown in Figure 12b. Increasing the amplification of the recording system gave the pattern shown in Figure 12c. To facilitate measurements of the recorder deflection as a function of distance in the cell the region of the trace corresponding to the solution column was enlarged by decreasing the scanning rate of the photomultiplier-slit assembly without altering the chart drive of the recorder. Only the relevant region of the trace is shown in Figure 12d. At this slow scanning rate (6 min to traverse the entire image) most of the high-frequency photomultiplier noise was eliminated by suitable adjustment of the electronic filter. In this manner smooth traces are produced without sacrificing resolution. The actual traces (corresponding to a 3-mm column of solution)

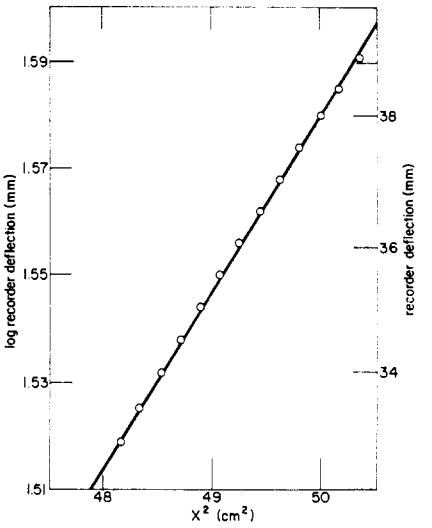

FIGURE 13: The determination of the molecular weight of adenosine by sedimentation equilibrium. On the ordinate is the logarithm of the recorder deflection in mm and the abscissa represents the square of the distance (cm^2) from the axis of rotation. The right-hand ordinate shows the actual recorder deflection on a logarithmic scale. The initial concentration of adenosine was 10 μg/ml and the solvent was 0.2 M NaCl. The rotor speed was 59,780 rpm and the data shown in the figure were measured on a trace obtained after 20 hr of centrifugation. The monochromator slit width was 2 mm and the wavelength was set at 265 mμ.

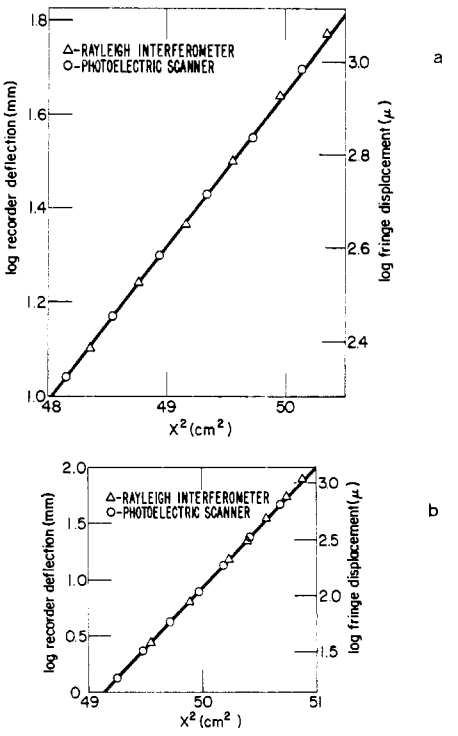

FIGURE 14: The molecular weight determination of bovine plasma albumin from sedimentation equilibrium experiments. Both Rayleigh interference patterns and traces from the photoelectric scanner were used for the measurements illustrated in the figure. The ordinate gives the logarithm of the recorder deflection (mm) on the left and the logarithm of the fringe displacement (μ) on the right. The abscissa shows the square of the distance (cm^2) from the axis of rotation. (a) Low-speed equilibrium: sedimentation was for 18 hr at 12,590 rpm. (b) High-speed equilibrium: sedimentation was for 22 hr at 24,630 rpm. For both experiments the solvent was 0.1 M NaCl and 0.01 M acetate at pH 5.4. The initial concentration of protein was 0.6 mg/ml.

are about 20 cm in length thereby permitting accurate measurements of recorder deflection to be made as a function of distance in the cell. Figure 12e shows the analogous trace when the amplification was increased.

With low molecular weight solutes such as adenosine the concentration change across the cell was very slight even at 60,000 rpm. Despite this, accurate data can be obtained for calculations of the molecular weight. This is illustrated by the plot in Figure 13 of the logarithm of the recorder deflection *vs.* the square of the distance from the axis of rotation. Combination of the slope of this plot with the partial specific volume, speed of the rotor, and temperature gave a molecular weight of 264 in excellent agreement with the known value of 267. In a second experiment with a slightly longer liquid column (to produce a larger concentration change throughout the solution) the molecular weight was 264.

In view of the excellent results with a low molecular weight material of known purity it seemed of interest to test the photoelectric scanner for molecular weight determinations of proteins which frequently are contaminated with higher aggregates. This afforded the opportunity also to assess the utility of the scanning system for the study of multicomponent systems and interacting systems involving association-dissociation equilibria.

Bovine Plasma Albumin. Figure 14 shows plots of the logarithm of concentration *vs.* the square of the distance from the axis of rotation in an experiment with bovine plasma albumin. To test the reliability of the photoelectric scanner the molecular weights were also evaluated from the Rayleigh interference patterns. As seen in both plots of Figure 14 excellent agreement was obtained for the concentration distribution determined with the two different optical systems. In the low-speed experiment illustrated by Figure 14a the weight-average molecular weight was 75,000. This particular sample contained appreciable amounts of dimers and higher aggregates (as seen in a sedimentation velocity experiment with schlieren optics). When the sedimentation equilibrium experiment was conducted at a higher centrifugal field (Yphantis, 1964) the

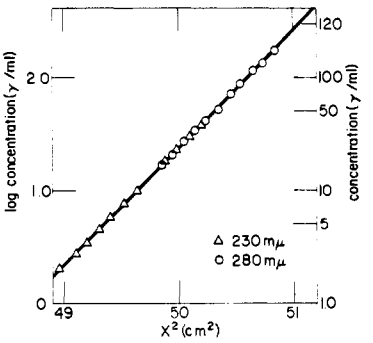

FIGURE 15: Molecular weight determinations of extremely dilute solutions by sedimentation equilibrium experiments. On the left ordinate is the logarithm of the concentration in μg/ml and on the right are the actual concentrations in μg/ml. These are plotted against the square of the distance (cm^2) from the axis of rotation. The data were obtained from traces recorded 18 hr after reaching the speed of 24,630 rpm. Two 7° cells were used in a single rotor with one cell containing the solvent and the other the solution. With this combination a long slit (10 mm) was used in the photomultiplier slit assembly. The switching circuit was activated by light pulses passing through the reference hole in the side of the rotor. Traces were produced with light of 280 mμ as indicated by ○ and also with light of 230 mμ represented by △. In both cases the slit width on the monochromator was 2 mm. Recorder deflections were converted to absolute concentrations with data obtained from independent calibration measurements.

aggregated molecules were preferentially concentrated near the cell bottom and the observed weight-average molecular weight of the principal component (Figure 14b) of 66,900 corresponded to the known value for albumin monomers.

Figures 14a and 14b illustrate the utility of the photoelectric scanning optical system for both low- and high-speed sedimentation equilibrium experiments. In effect absolute concentrations (which are directly proportional to recorder deflections) were measured directly from the traces. No recourse is needed to procedures such as those employed by Richards and Schachman (1959) or La Bar (1965) for identifying the interference fringes. At the same time the base-line problems described by Yphantis (1964) for high-speed sedimentation equilibrium experiments with interference optics are less serious when absorption optics are employed. In some experiments the bovine plasma albumin preparation was contaminated with ultraviolet light absorbing material of low molecular weight which was readily detected in the traces. Increasing the speed of the rotor to a value appropriate for a sedimentation velocity experiment caused the protein to be sedimented to the cell bottom thereby giving a trace for the "impurity." When this trace was employed as a "base line" for the equilibrium experiment the calculated molecular weight once again was in excellent agreement with the values obtained for the uncontaminated albumin.

The experiments illustrated by Figure 14 showed that accurate molecular weights were obtained when the photoelectric scanning system was used with light of 280 mμ. In these sedimentation equilibrium studies the maximum optical density (at the bottom of the cell) was about 1.1, corresponding for many proteins to concentrations of about 0.1–0.2 g/100 ml. The bulk of the experimental data employed in the molecular weight determinations corresponded to concentrations of about 0.01 g/100 ml. Although the concentrations required could be reduced somewhat (by a factor of 2.5) through the use of cells having a 30-mm optical path, it seemed more profitable to test the sensitivity and accuracy of the scanning system with light which is even more strongly absorbed by most proteins. Accordingly the very large peptide bond absorbance was exploited through the use of light having a wavelength of 230 mμ. Figure 15 represents the data from a high-speed sedimentation equilibrium experiment on bovine plasma albumin. For this experiment, after equilibrium was attained, traces were made with light of 280 and 230 mμ. As in the other high-speed equilibrium experiments the logarithm of the recorder deflection varied linearly with the square of the distance from the axis of rotation. The molecular weight calculated from the slope of the line was 64,500, in good agreement with the value deduced for the monomer in the experiment illustrated by Figure 14b.

Despite the difficulties imposed by working with light of wavelength about 230 mμ (Figure 15) the data obtained at that wavelength when converted to a concentration scale fell on the same straight line as those produced by the light of longer wavelength. As seen in the graph the two sets of data were complementary. At levels centripetal to the center of the liquid column the optical density (at 280 mμ) was so low (about 0.01) that the recorder deflection was less than 1 mm. Thus no reliable data could be obtained for that region of the cell if only light of 280 mμ were available. However, accurate measurements could be made from that region of the cell by decreasing the wavelength of the incident light to 230 mμ. At this wavelength the extinction coefficient (and recorder deflection) was increased sevenfold. As a consequence accurate data were obtained readily at concentrations as low as 4 μg/ml (corresponding to an optical density of 0.03 at 230 mμ). Near the bottom of the cell the absorbance at 230 mμ was so great that the response of the photoelectric scanner was no longer linear with concentration. Data for this region were obtained, therefore, with light of 280 mμ. The traces at the very bottom of the cell were exceedingly steep because of the high centrifugal field employed in the experiment. Therefore accurate data could not be obtained even though the concentration in that region was still within the range for which the recording system was linear.

The results presented in Figure 15 show that accurate molecular weights can be determined from sedimenta-

tion equilibrium experiments on protein solutions having concentrations of only 10 μg/ml. Since only 0.1 ml is required for an experiment, 1 μg will suffice for the evaluation. These results taken in conjunction with the data on adenosine and hemoglobin (*vide infra*) illustrate the remarkable sensitivity of the photoelectric scanning system for sedimentation studies on extremely dilute solutions.

Multicomponent Systems. Frequently the analysis of the subunit composition of proteins requires studies of the macromolecules in dissociating (and denaturing) solvents containing, in high concentrations, a third component such as guanidine hydrochloride (G-HCl) or urea (Schachman, 1960). These studies often are fraught with difficulty both experimentally and theoretically (Williams *et al.*, 1958; Schachman, 1959; Fujita, 1962). It is not our intention here to treat this problem in detail but rather to show the utility of the photoelectric scanner for such experiments. The major experimental pitfall in sedimentation studies of proteins in 5 M G-HCl solutions, for example, resides in the inability of refractometric or interferometric optical methods to distinguish optical contributions of the protein molecules from those due to the G-HCl. This is especially hazardous since generally the protein concentrations are very low and the third component is present in very high concentrations. Even with double-sector cells difficulties arise because of imperfectly matched menisci and possible preferential interactions between the macromolecules and either of the two components of the mixed solvent (Williams *et al.*, 1958). This ambiguity can be circumvented completely with absorption optics if light of the appropriate wavelength is used. In this way the concentration distribution of the macromolecules is measured independent of any concentration gradients of the third component (Schachman, 1959, 1963b).

Figure 16 shows the sedimentation equilibrium patterns for aldolase in 3, 5, and 7 M G-HCl solutions. These were obtained in a single experiment by placing the three samples along with the analogous solvents in the appropriate compartments of a multicompartment double-channel cell (Yphantis, 1964). At 280 mμ the G-HCl solutions were virtually transparent and no special precautions were taken in filling the cells to have the menisci in the conjugate compartments at the same levels. From the traces, plots were made of the logarithm of recorder deflection *vs.* the square of the distance from the axis of rotation. These are shown in Figure 17a–c. The slopes of these lines after suitable correction for the rotor speed and absolute temperature give values for $M_e(1 - \bar{V}_e\rho)$ where M_e and $\bar{V}_e$ refer to the molecular weight and partial specific volume of the complex between the protein and the preferentially bound low molecular weight constituent. In the absence of any preferential interactions a correct value of the molecular weight of the polypeptide chains is obtained by substitution of the partial specific volume of the protein in the mixed solvent. For this special case the theory reduces to that of a two-component system and the mixed solvent is treated as a single component. When preferential interactions occur, however, the evaluation of molecular weights is more difficult, and two different procedures are available.

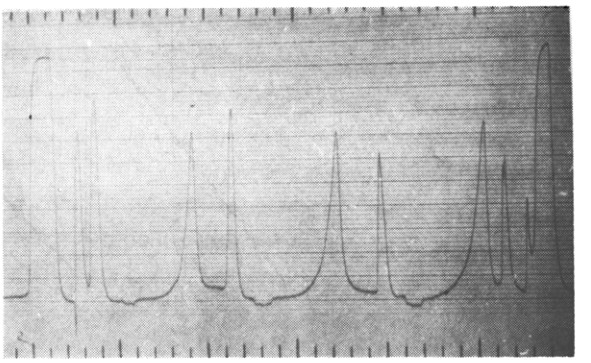

FIGURE 16: Recorder traces illustrating the sedimentation equilibrium patterns produced by the photoelectric scanning system when used with a multicompartment (Yphantis) cell. The sample compartments contain, from left to right, aldolase at 0.5 mg/ml in 3, 5, and 7 M G-HCl. The solvent compartments contained the corresponding G-HCl solutions. The recorder traces were obtained after sedimentation for a period of 48 hr at 34,020 rpm. Light with a wavelength of 280 mμ was used and the slit width on the monochromator was 2 mm.

On the one hand the partial specific volume of the complex must be determined and then combined with that of the polypeptide chains to provide quantitative information of the composition of the complex (*i.e.*, the amount of H_2O or G-HCl preferentially bound per gram of protein). With these data the correct molecular weight is calculated readily (Williams *et al.*, 1958; Schachman, 1959, 1960; Fujita, 1962). Alternatively the molecular weight of the protein can be calculated without evaluating the preferential interaction by using a special definition of the components and determining the partial specific volume from density measurements on the dialyzed solutions of the protein (and the dialysates) (Casassa and Eisenberg, 1960, 1961, 1964). A detailed comparison of these two approaches will appear elsewhere; our purpose here is solely to illustrate, in a preliminary way, the potential of the photoelectric scanning system for the evaluation of preferential interactions and the determination of molecular weights of protein subunits in concentrated G-HCl solutions.

For the three G-HCl solutions of aldolase the values of $M_e(1 - \bar{V}_e\rho)$ were respectively 10,070, 7820, and 5590. When these were plotted *vs.* the densities of the appropriate G-HCl solutions, a straight line resulted as shown in Figure 17d. Extrapolation of the data to a value of $M_e(1 - \bar{V}_e\rho) = 0$ gave 1.29 g/ml as the density of a hypothetical G-HCl solution in which there would be no redistribution of the protein subunits. The reciprocal of this value represents the partial specific volume of the protein complex in the mixed solvent.

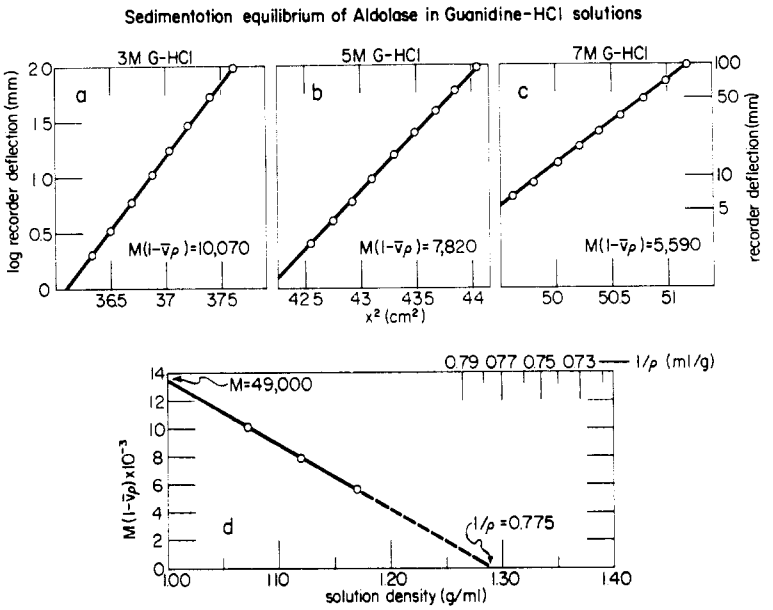

FIGURE 17: Sedimentation equilibrium of aldolase in G-HCl solutions. The upper three graphs represent the logarithm of the recorder deflection (mm) on the left ordinate and the recorder deflection (mm) on the right ordinate *vs.* the square of the distance from the axis of rotation (cm^2) on the abscissa. The graphs at the top, a–c, correspond to 3, 5, and 7 M G-HCl, respectively. In the lower graph, d, are plotted the slopes from the upper figures after correction to give $M(1 - \bar{V}\rho)$ *vs.* the densities of the various solutions. A straight line is drawn through the data along with an extrapolation to the value of the ordinate corresponding to $\rho = 1$ and a value of the abscissa representing $M(1 - \bar{V}\rho) = 0$. For translating the value of ρ corresponding to zero redistribution into its equivalent of partial specific volume, the abscissa for the lower figure is converted to the reciprocal value, $1/\rho$, on the upper part of that figure. The experimental conditions for this experiment are described in the legend to Figure 16.

Since this value, 0.775 ml/g, is significantly higher than the partial specific volume of aldolase, 0.742 ml/g (Taylor and Lowry, 1956), water must be bound preferentially to the unfolded polypeptide chains to the extent of 0.14 g of H_2O/g of protein. No allowance was made in this estimation of the preferential interaction for any possible decrease in the partial specific volume of the protein upon denaturation in G-HCl (Linderstrøm-Lang, 1952; Kielley and Harrington, 1960; Woods *et al.*, 1963; Reithel and Sakura, 1963; Marler *et al.*, 1964). If the partial specific volume of the polypeptide chains decreased to 0.73 ml/g the calculated preferential interaction would amount to 0.20 g of H_2O/g of protein. With the assumption that the partial specific volume of the complex (and hence the preferential interaction) is independent of the concentration of G-HCl, the molecular weight of the disorganized polypeptide chains, M_p, is readily calculated from the values of $M_c(1 - \bar{V}_c\rho)$ and the value of V_c 0.775 ml/g, after correcting for the preferentially bound water, x, according to $M_c = M_p(1 + x)$. The results obtained in this way (using a value of 0.73 ml/g for $\bar{V}$) were 50,000, 49,500 and 49,900 for the 3, 5, and 7 M G-HCl solutions, respectively. A similar value, 49,600, was obtained for the molecular weight of the subunits by extrapolating the data of Figure 17d to $\rho = 1.0$. Under these circumstances the effects due to any preferential interactions would vanish.

In the particular experiments illustrated by Figure 17 the extrapolations to $M_c(1 - \bar{V}_c\rho) = 0$ and $\rho = 1.0$ seem hazardous because of the limited data, but results with aldolase and other proteins in different mixed solvents lend support to the procedure outlined above. It should be noted that the quantity, $M_c(1 - \bar{V}_c\rho)$, may vary with ρ in a linear fashion, as in Figure 17d, even though $\bar{V}_c$ is not a constant. This possibility cannot be excluded by the type of experiment presented here. Despite this uncertainty, however, sedimentation equilibrium studies of this type provide a reliable indication of possible preferential interactions in multicomponent systems. They should be compared with the somewhat analogous experiments in which the sedimentation coefficient (corrected for the viscosity of the mixed solvent) is plotted *vs.* the density (Schachman and Lauffer, 1949; Lauffer and Bendet, 1954; Cox and Schumaker 1961a,b; Schumaker and Cox, 1961; Hill and Cox, 1965). Clearly the equilibrium experiments are to be preferred on theoretical grounds over the sedimentation velocity studies (Peller, 1958). These preliminary equilibrium studies indicate that this approach is preferable also from an experimental viewpoint since viscosity data are not required, smaller amounts of the macromolecular solute are needed, and the results are not as dependent on accurate knowledge of the temperature as are sedimentation velocity measurements.

The preliminary results presented here show the importance of attempts to evaluate possible preferential interactions in multicomponent systems. Without corrections of this type the calculated molecular weights of the subunits would have been 46,600, 43,000, and 38,300 for the 3, 5, and 7 M G-HCl solutions, respectively.[2] Much work remains to be done to provide further validation of the approach described here; in particular a comparison is needed with the procedure suggested by Casassa and Eisenberg (1964). In the meantime the findings serve to emphasize that tacit assumptions regarding the absence or unimportance of preferential interactions in G-HCl are unwarranted.

Comparable sedimentation equilibrium experiments on proteins in H_2O–D_2O solutions showed that the procedure illustrated by Figure 17 can yield accurate values for the partial specific volumes (S. J. Edelstein and H. K. Schachman, in preparation). For this type of system preferential interactions are apparently negligible and corrections need be made only for deuterium exchange. This procedure shows promise as an accurate technique for determining partial specific volumes with only microgram quantities being required.

Associating–Dissociating Systems. In view of the sensitivity of the photoelectric scanning system it seemed of interest to assess the value of this optical method for the study of the association–dissociation behavior of human oxyhemoglobin. Accordingly both sedimentation velocity and equilibrium experiments were conducted on oxyhemoglobin. As a control and test of the validity of the experimental results, limited studies were performed on sperm whale myoglobin.

Figure 18 shows the results from a sedimentation equilibrium experiment on oxyhemoglobin in 0.1 M phosphate buffer at pH 7.0. The initial concentration was 0.025 mg/ml corresponding to an optical density of 0.2 at 405 mμ. Unlike the experiments described above the plot of the logarithm of the recorder deflection *vs.* the square of the distance from the axis of rotation showed marked upward curvature. Such an observation is characteristic of an association–dissociating system or a polydisperse mixture of noninteracting components. The latter alternative was eliminated as a result of sedimentation velocity experiments at various concentrations which showed that the sedimentation coefficient of the single boundary increased progressively from 2.0 S at 0.002 mg/ml to 4.6 S at 0.25 mg/ml. In addition the molecular weights calculated from the tangents to the concentration–distance curves (such as Figure 18) were a function only of the concentration and independent of rotor speed. Such behavior is characteristic of chemically reacting systems involving association–dissociation equilibria.

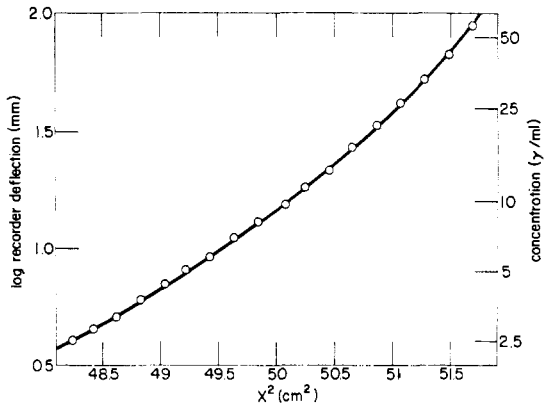

FIGURE 18: Molecular weight determination of human oxyhemoglobin from sedimentation equilibrium experiments. The left ordinate gives the logarithm of the recorder deflection (mm) and the right ordinate gives the protein concentration directly in μg/ml. The abscissa represents the square of the distance (cm^2) from the axis of rotation. The initial concentration of the oxyhemoglobin was 0.025 mg/ml and the solution was sedimented for 24 hr at 24,630 rpm in a buffer containing 0.1 M phosphate at pH 7.0. The traces were recorded with light having a wavelength of 405 mμ.

The results from a series of experiments are shown in Figure 19 as a plot of molecular weight as a function of concentration. Some of the data were obtained from a single experiment (such as that represented by Figure 18). Measurements were made at different levels in the cell corresponding to different average concentrations. To facilitate experimentation at the lowest concentrations a rotor speed of 47,040 rpm was employed. In this way average molecular weights were determined at concentrations from 0.0026 to 0.01 mg/ml. At this speed the concentration gradient at the cell bottom was so large as to preclude accurate molecular weight measurements at higher concentrations. With a rotor speed of 24,630 rpm (for the same solution) this difficulty was obviated. Through the use of different speeds a series of molecular weights was obtained over a broad concentration range in a single experiment. At concentrations above 0.05 mg/ml, the absorbance at 405 mμ was too high; accordingly light of 540 mμ was employed and the rotor speed was lowered to 15,720 rpm since the average molecular weight at that concentration was about 60,000. The data at the

[2] It is of interest that these experimental results, uncorrected for possible preferential interactions, are in agreement with the recent experiments of Kawahara and Tanford (1966) for aldolase in 6 M G-HCl. Since their experiments were performed at only one concentration of G-HCl, the trend shown above was not detected. Moreover these workers did not consider the possible complications of multicomponent theory and by using the experimental result of 40,000 for the molecular weight of the polypeptide chains, they were led to the conclusion that aldolase is composed of four chains. This conclusion is at variance with that deduced earlier from sedimentation equilibrium experiments on aldolase in other denaturing media as well as end-group determinations (Stellwagen and Schachman, 1962; Deal *et al.*, 1963; Hass and Lewis, 1963; Hass, 1964; Drechsler *et al.*, 1959; Kowalsky and Boyer, 1960; Winstead and Wold, 1964). A detailed demonstration of the existence of three polypeptide chains in aldolase will be presented elsewhere (S. J. Edelstein, F. Hamburg, and H. K. Schachman, in preparation).

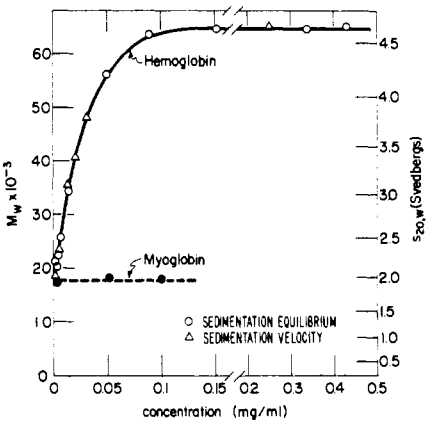

FIGURE 19: Molecular weights and sedimentation coefficients as a function of concentration for human oxyhemoglobin and sperm whale myoglobin. The left ordinate gives the weight-average molecular weight as determined by sedimentation equilibrium and the right ordinate represents the sedimentation coefficient in svedbergs. The scale for the sedimentation coefficient was adjusted so that a value of 4.6 S corresponded to a molecular weight of 64,000 and the values of s were proportional to $M^{2/3}$. Sedimentation coefficients are indicated by △ and molecular weights are represented by ○. The concentrations are given on the abscissa in mg/ml. Data at concentrations below 0.05 mg/ml were obtained with light at 405 mμ and measurements with more concentrated solutions were made with light having a wavelength of 540 mμ. For the sedimentation equilibrium experiments speeds of 9945 rpm to 47,040 rpm were employed. All sedimentation velocity experiments were conducted at 59,780 rpm.

highest concentrations were obtained with a cell having an optical path of only 3 mm so that the optical densities at the bottom were still within the range of the linear response of the recording system.

In order to permit a comparison of the molecular weight data with the measured average sedimentation coefficients over the same range of concentrations both sets of results are given in Figure 19. The scale for the sedimentation coefficients was adjusted so that the value 4.6 S (obtained at concentrations of 0.25 mg/ml and above) corresponded to a molecular weight of 64,000. In addition the restriction was imposed that sedimentation coefficients of globular molecules are proportional to (molecular weight)$^{2/3}$. At the very low concentrations employed in these studies the sedimentation coefficient observed for oxyhemoglobin approached the value, 1.8 S, found for myoglobin.

The results presented in Figure 19 demonstrate clearly that oxyhemoglobin dissociates into single chains when the concentration is decreased to about 3×10^{-5} M. As seen in Figure 19 the molecular weight of oxyhemoglobin at these low concentrations is about the same as that observed for sperm whale myoglobin. For the latter the molecular weight was independent of concentration; over the range examined, concentration effects due to nonideality are so small as to be undetectable. It is well known that the four-chain hemoglobin molecules are in dynamic equilibrium with two-chain molecules (Rossi-Fanelli *et al.*, 1964; Wyman, 1964; Benesch *et al.*, 1965; Kirshner and Tanford, 1964; Kawahara *et al.*, 1965; Ackers and Thompson, 1965) with the dissociation being affected by the pH, ionic strength, the nature of the ligand at the iron atom, and the presence of specific ions. In some studies depending upon the conditions (Guidotti and Craig, 1963; Guidotti *et al.*, 1963; Ansevin and Yphantis, 1964;) dissociation into single-chain molecules occurred at low concentrations of hemoglobin. It should be noted, however, that in none of these earlier investigations were the concentrations as low as those employed in the experiments described here. Therefore complete dissociation of oxyhemoglobin into single α and β chains as demonstrated here could not have been detected by the methods used heretofore. Although the results shown in Figure 19 are of use in considerations of the dissociation of the tetrameric structure of hemoglobin into monomers, they are presented here primarily to demonstrate the potential of the split-beam photoelectric scanner in the study of association-dissociating systems.[3]

Discussion

During the initial phases of the development of the split-beam scanner emphasis was directed toward the design of a convenient, versatile photoelectric optical system capable of discriminating among various chemical species on the basis of differences in their absorption spectra. Although these goals were achieved in the earlier versions (Hanlon *et al.*, 1962; Schachman *et al.*, 1962; Lamers *et al.*, 1963) considerable modifications were required in order to increase the accuracy and sensitivity of the photoelectric scanning absorption optical system. These changes took various forms. By incorporating a power supply for the logarithmic compressor and a feed-back regulator to control the voltage applied to the photomultiplier the range of linearity of the recording system was enhanced and spurious switching signals eliminated. Drift was reduced substantially by suitable changes in the electronic circuitry and components. The most significant gain in sensitivity resulted from the incorporation of the

[3] Calculation of equilibrium constants from these data would be premature since no effort was made to evaluate systematically the variation of molecular weight with concentration by fitting a continuous function to the data from a single experiment (Jeffrey and Coates, 1966). Nor was there an attempt to combine overlapping data from experiments at different speeds and initial concentrations (Yphantis, 1964). In addition, temperature was not controlled precisely but maintained only by refrigeration as described earlier. Subsequent communications (S. J. Edelstein and H. K. Schachman, in preparation) will treat equilibrium constants for hemoglobin under different conditions and at various degrees of oxygen saturation so as to provide some insight regarding the strength of interchain bonding and the relationship between subunit association-dissociation equilibria and oxygen binding.

stationary photomultiplier which in conjunction with modified electronic circuits and longer slits in front of the scanning photomultiplier permitted the use of 7° single-sector cells separated by 180°. As described and illustrated above this provided an opportunity also to analyze two solutions in a single ultracentrifuge experiment by employing two double-sector cells. The modification of the electronic circuits also provided an opportunity to eliminate most of the speed dependence of the recording system. In the earlier version the net recorder deflection per unit optical density difference between the solvent and solution varied appreciably with rotor speed. This represented a serious limitation because it precluded accurate measurements of the amount of light-absorbing solute which sedimented to the bottom of the cell as the rotor was accelerated to the desired speed. With the addition of the electronic calibrating circuit which compares the attentuation of the light beam caused by the solution (relative to the solvent) with a known electrical attentuation, absolute optical densities are measured readily.

Although the electronic components of the split-beam scanner function effectively it is important to note that the photoelectric unit, like any spectrophotometer, is vulnerable to the effects of stray light. Without masks on the collimating and condensing lenses of the vacuum chamber both compartments of the double-sector cell are imaged simultaneously by the camera lens. Due to imperfections in the latter, reflections from all optical surfaces, and scattering of light from oil and dust deposits on the lenses in the vacuum chamber these images overlap partially at the plane of the photomultiplier slit. As a consequence in experiments with solutions of high optical density the photomultiplier "sees" light when none should be detected. A substantial improvement has been made by the incorporation of two adjustable masks on the vacuum chamber lenses and a third on the top of the optical track just below the 45° front-surfaced mirror. Still further gains doubtless could be achieved by the incorporation of additional masks to eliminate remaining reflections.

The experience gleaned from the use of the split-beam photoelectric scanner indicates numerous directions for further improvements. The logarithmic convertor should be replaced with one having a greater range of linearity. Although the recorder used in this work is ideal for sedimentation velocity experiments, a unit having a longer pen travel and greater accuracy and linearity is desirable for sedimentation equilibrium studies. In this regard the incorporation of the multi-speed transmission for the photomultiplier-slit assembly has proven especially valuable in permitting measurements of the concentration distribution at sedimentation equilibrium from 6-min traces. More intense, stable light sources with greater lifetimes are needed. At present there is considerable variation among presumably identical sources and for each of them the cooling fan has to be adjusted so as to produce optimal light levels for the wavelengths desired. For this purpose an oscilloscope which portrays directly the output of the photomultiplier is indispensable. Monitoring the light pulses with the oscilloscope, and thereby bypassing all of the electronic circuits, permits the ready detection of malfunctioning components in the photoelectric optical system as well as leaks between the two compartments of the double-sector cell. As longer slits are employed in the scanning photomultiplier assembly the straight slits should be replaced by curved slits. In this way resolution would be enhanced since the curvature at the detecting element would be compatible with the cylindrical shape of the concentration gradients in the ultracentrifuge cells. To exploit longer slits at the photomultiplier cells of greater sector angle are needed. These can be obtained by shortening the cells in the radial direction. Such cells, though impractical for sedimentation velocity experiments, would be useful in sedimentation equilibrium studies. In view of the successful performance of the photoelectric scanning system it seems appropriate now to consider incorporating facilities for direct, digital recording on tape. This could take various forms any of which would be compatible with the requirements of high-speed digital computers.

As shown in both sedimentation velocity and equilibrium experiments the concentration range available for study has been increased greatly through the use of the photoelectric scanner. Studies of proteins at a concentration of only a few micrograms per milliliter are now routine. The observation that ATCase does not dissociate at 3 μg/ml is particularly significant since it provides an indication of the strength of the noncovalent attractive forces among the subunits in this enzyme (Gerhart and Schachman, 1965). In contrast human oxyhemoglobin at comparable concentrations is almost completely dissociated into its constituent polypeptide chains even under conditions of pH and ionic strength which are considered generally to favor the four-chain structure. By combined velocity and equilibrium studies in conjunction with the appropriate theory, it should be possible to elucidate the amounts of the various molecular species present at various concentrations. From such data the appropriate thermodynamic quantities can be evaluated.

It should be noted that calculations of the molecular weight from the scanner traces are very simple as compared, for example, with those required when interference optical systems are employed. Base-line problems due to cell distortions are of little consequence when the scanner is used, whereas they are serious in molecular weight calculations from interference patterns. Because of the self-plotting feature of the photoelectric scanner anomalies such as convection in the sedimentation experiments may be detected directly. By stationing the photomultiplier-slit assembly at a position in the image plane corresponding to the air–liquid meniscus in one compartment of the cell or at the edge of the reference hole in the counterbalance cell it is possible to detect vibrations or precessions of the rotor. This provides an extremely sensitive test of the performance of ultracentrifuge drives since the light striking the photomultiplier depends on minute movements of the rotor in a radial direction.

The photoelectric scanning absorption system is particularly useful in the study of multicomponent systems. By judicious selection of the wavelength of the incident light the redistribution of the various components can be measured at will. This has been illustrated elsewhere (Schachman, 1960, 1963a; Schachman *et al.*, 1962) and detailed sedimentation equilibrium studies of interacting systems involving large and small molecules will be described elsewhere (I. Z. Steinberg and H. K. Schachman, in preparation). The results presented above illustrate the application of the scanner for the study of proteins in the presence of high concentrations of denaturing agents such as G-HCl. Whereas the photomultiplier "sees" only the protein without contributions from the third component, the contributions from the latter dominate when refractometric or interferometric optical systems are employed. If suitable precautions are not taken when the schlieren or Rayleigh optical systems are used for such systems, serious errors may occur in molecular weight determinations.

As shown in Figures 13–15 the photoelectric scanner is equally suited for the analysis of data from both low- and high-speed sedimentation equilibrium experiments. Because the recorder deflection is directly proportional to optical density (or solute concentration) and the instrument is nulled at the outset to indicate zero concentration (in the air space of the cell or with a special counterbalance), the absolute value of the concentration is measured directly and simply at any level in the solution column. There is no need to have centrifugal fields of sufficient magnitude to cause the solute concentration near the meniscus to approach zero. Nor is there a need for special computational procedures based on the conservation of mass. This is perhaps one of the greatest virtues of the photoelectric scanning absorption system relative to other optical systems. The absorption system is not free of pitfalls, however. Its sensitivity constitutes a potential hazard; consequently impurities of high extinction coefficient may give misleading results if precautions are not taken. This difficulty can be overcome in part at least by examination of equilibrium patterns obtained with light of various wavelengths. In this way impurities can be detected and appropriate corrections made for their contribution to the over-all pattern. Also it should be noted that convective disturbances are more likely to occur when dilute solutions are employed in ultracentrifuge experiments (*cf.* Schachman, 1959; Yphantis, 1964). By the use of high centrifugal fields as recommended by Yphantis (1964), low temperatures, and by disconnecting the heater in the vacuum chamber, convective disturbances can be reduced substantially. The presence of a low molecular weight, transparent solute such as salt or sucrose is particularly valuable in providing a stabilizing density gradient.

Acknowledgment

It is a pleasure to express our indebtedness and thanks to K. Lamers, R. Johnson, G. Lauterbach, and A. Stern for their innumerable contributions in the design and construction of the electronic circuitry and the mechanical equipment. We are grateful also to L. Gropper for many suggestions and valuable discussions. His proposal of the use of the PEK light source and cooperation in modifying the light source compartment of the monochromator have been most helpful. Valuable ideas were also contributed by W. Boyd and S. Rasmussen based on their own experience in constructing an analogous instrument.

References

Ackers, G. K., and Thompson, T. E. (1965), *Proc. Natl. Acad. Sci. U. S. 53*, 342.

Ansevin, A. T., and Yphantis, D. A. (1964), Abstracts, Biophysical Society, WB12, Feb 26–28, 1964, Chicago, Ill.

Aten, J. G. T., and Schouten, A. (1961), *J. Sci. Instr. 38*, 325.

Benesch, R. E., Benesch, R., and MacDuff, G. (1965), *Proc. Natl. Acad. Sci. U. S. 54*, 535.

Bessman, J. J., Lehman, I. R., Adler, J., Zimmerman, S., Simms, E. S., and Kornberg, A. (1958), *Proc. Natl. Acad. Sci. U. S. 44*, 633.

Casassa, E. F., and Eisenberg, H. (1960), *J. Phys. Chem. 64*, 753.

Casassa, E. F., and Eisenberg, H. (1961), *J. Phys. Chem. 65*, 427.

Casassa, E. F., and Eisenberg, H. (1964), *Advan. Protein Chem. 19*, 287.

Cheng, P. Y., and Littlepage, J. L. (1966), *Anal. Biochem. 15*, 211.

Cox, D. J., and Schumaker, V. N. (1961a), *J. Am. Chem. Soc. 83*, 2433.

Cox, D. J., and Schumaker, V. N. (1961b), *J. Am. Chem. Soc. 83*, 2439.

Dayhoff, M. D., Perlman, G. E., and MacInnes, D. A. (1952), *J. Am. Chem. Soc. 74*, 2515.

Deal, W. L., Rutter, W. F. and Van Holde, K. E. (1963), *Biochemistry 2*, 246.

Deschepper, J. C., and Van Rapenbush, R. (1964), *Compt. Rend. 258*, 5999.

Drechsler, E. R., Boyer, P. D. and Kowalsky, A. G. (1959), *J. Biol. Chem. 234*, 2627.

Fujita, H. (1962), Mathematical Theory of Sedimentation Analysis, New York, N. Y., Academic.

Gerhart, J. C., and Schachman, H. K. (1965), *Biochemistry 4*, 1054.

Guidotti, G., and Craig, L. C. (1963), *Proc. Natl. Acad. Sci. U. S. 50*, 46.

Guidotti, G., Konigsberg, W., and Craig, L. C. (1963), *Proc. Natl. Acad. Sci. U. S. 50*, 774.

Hanlon, S., Lamers, K., Lauterbach, G., Johnson, R., and Schachman, H. K. (1962), *Arch. Biochem. Biophys. 99*, 157.

Harrington, W. F., and Schellman, J. A. (1956), *Compt. Rend. Trav. Lab. Carlsberg 30*, 21.

Hartley, R. W., Peterson, E. Z., and Sober, H. A. (1962), *Biochemistry 1*, 60.

Hass, L. F. (1964), *Biochemistry 4*, 535.

Hass, L. F. and Lewis, M. S. (1963), *Biochemistry 2*, 1368.
Hill, J., and Cox, D. J. (1965), *J. Phys. Chem. 69*, 3032.
Jeffrey, P. D., and Coates, J. H. (1966), *Biochemistry 5*, 489.
Kawahara, K., Kirshner, A. G., and Tanford, C. (1965), *Biochemistry 4*, 1203.
Kawahara, K., and Tanford, C. (1966), *Biochemistry 5*, 1578.
Kielly, W. W., and Harrington, W. F. (1960), *Biochim. Biophys. Acta 47*, 462.
Kirshner, A. G., and Tanford, C. (1964), *Biochemistry 3*, 291.
Kowalsky, A. and Boyer, P. D. (1960), *J. Biol. Chem. 235*, 604.
LaBar, F. E. (1965), *Proc. Natl. Acad. Sci. U. S. 54*, 31.
Lamers, K. (1965), University of California Lawrence Radiation Laboratory Publication, UCRL-11623.
Lamers, K., Putney, F., Steinberg, I. Z., and Schachman, H. K. (1963), *Arch. Biochem. Biophys. 103*, 379.
Lauffer, M. A., and Bendet, I. J. (1954), *Advan. Virus Res. 2*, 241.
Linderstrøm-Lang, K. U. (1952), Lane Medical Lectures: Proteins and Enzymes, Stanford, Calif., Stanford Univ. Press.
Marler, E., Nelson, C. A., and Tanford, C. (1964), *Biochemistry 3*, 279.
Peller, L. (1958), *J. Chem. Phys. 29*, 415.
Perlmann, G. E., and Longsworth, L. G. (1948), *J. Am. Chem. Soc. 70*, 2719.
Reithel, F. J., and Sakura, J. D. (1963), *J. Phys. Chem. 67*, 2497.
Richards, E. G., and Schachman, G. K. (1957), *J. Am. Chem. Soc. 79*, 5324.
Richards, E. G., and Schachman, H. K. (1959), *J. Phys. Chem. 63*, 1578.
Rossi-Fanelli, A., Antonini, E., and Caputo, A. (1964), *Advan. Protein Chem. 19*, 73.
Schachman, H. K. (1959), Ultracentrifugation in Biochemistry, New York, N. Y., Academic.
Schachman, H. K. (1960), *Brookhaven Symp. Biol. 13*, 49.
Schachman, H. K. (1963a), *Biochemistry 2*, 887.
Schachman, H. K. (1963b), *in* Ultracentrifugal Analysis in Theory and Experiment, Williams, J. W., Ed., New York, N. Y., Academic, p 171.
Schachman, H. K., Gropper, L., Hanlon, S., and Putney, F. (1962), *Arch. Biochem. Biophys. 99*, 175.
Schachman, H. K., and Lauffer, M. A. (1949), *J. Am. Chem. Soc. 71*, 536.
Schumaker, V. N., and Cox, D. J. (1961), *J. Am. Chem. Soc. 83*, 2455.
Schumaker, V. N., and Schachman, H. K. (1957), *Biochim. Biophys. Acta 23*, 628.
Shooter, K. V., and Butler, J. A. V. (1956), *Trans. Faraday Soc. 52*, 734.
Spragg, S. P., Travers, S., and Saxton, T. (1965), *Anal. Biochem. 12*, 259.
Stellwagen, E. and Schachman, H. K. (1962), *Biochemistry 1*, 1056.
Svedberg, T., and Pedersen, K. O. (1940), The Ultracentrifuge, New York, N. Y., Oxford Univ. Press.
Taylor, J. F., Green, A. A., and Cori, G. T. (1948), *J. Biol. Chem. 173*, 591.
Taylor, J. F., and Lowry, C. (1956), *Biochim. Biophys. Acta 20*, 109.
Theorell, H. (1934), *Biochem. Z. 268*, 46.
Van Holde, K. E., and Baldwin, R. L. (1958), *J. Phys. Chem. 62*, 734.
Van Rapenbush, R., and Deschepper, J. C. (1966), *Compt. Rend. 262*, 1365.
Williams, J. W., Van Holde, K. E., Baldwin, R. L., and Fujita, H. (1958), *Chem. Rev. 58*, 715.
Winstead, J. A., and Wold, F. (1964), *J. Biol. Chem. 239*, 4212.
Woods, E. F., Himmelfarb, S., and Harrington, W. F. (1963), *J. Biol. Chem. 238*, 2374.
Wyman, J. Jr. (1964), *Advan. Protein Chem. 19*, 223.
Yphantis, D. A. (1964), *Biochemistry 3*, 297.